Dynamics of the North American Ice Sheet Complex during its inception and build-up to the Last Glacial Maximum

Chris R. Stokes[1][*], Lev Tarasov[2] and Arthur S. Dyke[3][, 4]

[1]*Department of Geography, Durham University, Durham, DH1 3LE, UK*
[2]*Department of Physics and Physical Oceanography, Memorial University of Newfoundland, St. John's, Newfoundland, Canada, A1B 3X7*
[3]*Geological Survey of Canada, 601 Booth St., Ottawa, Ontario, Canada, K1A 0E8*
[4]*Department of Geography, Memorial University of Newfoundland, St John's, Newfoundland, Canada, A1B 3X7*

*Corresponding author: Tel. +44 (0)191 334 1955; Fax. +44 (0191) 334 1801
E-mail address: c.r.stokes@durham.ac.uk (C R Stokes)

Keywords: North American Ice Complex; ice sheet; Laurentide Ice Sheet, numerical modelling; ice streams

Abstract: The North American Ice Sheet Complex played a major role in global sea level fluctuations during the Late Quaternary but our knowledge of its dynamics is based mostly on its demise from the Last Glacial Maximum (LGM), a period characterised by non-linear behaviour in the form of punctuated ice margin recession, episodic ice streaming and major shifts in the location of ice divides. In comparison, knowledge of the pre-LGM ice complex is poorly constrained, largely because of the fragmentary nature of the evidence relating to ice sheet build-up. In this paper, we explore the inception and growth of ice (120-20 ka) using a glacial systems model which has been calibrated against a large and diverse set of data relating to the deglacial interval. We make use of calibration data prior to the LGM but its scarcity introduces greater uncertainty, which is partly alleviated by our large ensemble

27   analysis. Results suggest that, following the last interglaciation (Oxygen Isotope Stage: OIS

28   5e), the ice complex initiated over the north-eastern Canadian Arctic and in the Cordillera

29   within a few thousand years. It then underwent rapid growth to an OIS 5 maximum at ~110

30   ka (5d) and covered ~70% of the area occupied by the LGM ice cover (although only 30% by

31   volume). An OIS 5 minimum is modelled at ~80 ka (5a), before a second phase of rapid

32   growth at the start of OIS 4, which culminated in a large ice complex at ~65 ka (almost as

33   large as at the LGM). Subsequent deglaciation was rapid (maximum modelled sea level

34   contribution of >16 cm per century) and resulted in an OIS 3 minimum between ca. 55-60 ka.

35   Thereafter, the ice complex grew towards its LGM configuration, interrupted by several

36   phases of successively less significant mass loss. Our results support and extend previous

37   inferences based on geological evidence and reinforce the notion of a highly dynamic pre-

38   LGM ice complex (e.g. with episodes of ± 10s m of eustatic sea level equivalent in <5 ka).

39   Consistent with previous modelling, the fraction of warm-based ice increases towards the

40   LGM from <20 to >50%, but even the thin OIS 5 ice sheets exhibit fast flow features (several

41   1000 m a^{-1}) in major topographic troughs. Notwithstanding the severe limitations imposed by

42   the use of the 'shallow-ice approximation', we note that most fast flow-features generated

43   prior to the LGM correspond to the location of 'known' ice streams during deglaciation, i.e.

44   in major topographic troughs and over soft sediments at the southern and western margins.

45   Moreover, the modelled flux of these 'ice streams' (*sensu lato*), appears to be non-linearly

46   scaled to ice sheet volume, i.e. there is no evidence that decay phases were associated with

47   significantly increased ice stream activity. This hypothesis requires testing using a model

48   with higher-order physics and future modelling would also benefit from additional pre-LGM

49   constraints (e.g. dated ice free/margin positions) to help reduce and quantify uncertainties.

50

51

52

1. Introduction

The North American Ice Sheet Complex (NAISC) includes the Laurentide, Cordilleran and Innuitian Ice Sheets and other smaller ice caps (e.g. in Newfoundland and the Appalachians) and was the largest ice mass to grow and (almost) completely disappear during the last glacial cycle, thereby playing a major role in Late Pleistocene sea level change (Fulton and Prest, 1987; Shackleton, 1987; Lambeck and Chapell, 2001; Cutler *et al*., 2003). Our knowledge of its extent and dynamics, however, is based largely on reconstructions of its deglaciation since the Last Glacial Maximum (LGM), for which we now have a moderately well-constrained ice margin chronology in most, but not all, sectors (e.g. Dyke and Prest, 1987; Dyke *et al*., 2003; Dyke, 2004; Clark *et al.*, 2009). Moreover, reconstructions of its behaviour during deglaciation attest to its dynamism and reveal major shifts in the location of ice divides (e.g. Dyke and Prest, 1987; Clark *et al*., 2000; Tarasov *et al*., 2012); episodes of ice streaming (e.g. Patterson, 1997; 1998; Winsborrow *et al.* 2004; Stokes *et al*., 2009) switches in ice sheet basal thermal regime (e.g. Dyke and Morris, 1988; Kleman and Hättestrand, 1999; Kleman and Glasser, 2007; Tarasov and Peltier, 2007) and abrupt episodes of mass loss that likely contributed to 'meltwater pulses' identified in the global sea level record (e.g. Hesse and Khodabakhsh, 1998; Hesse *et al*., 2004; Hemming, 2004; Tarasov and Peltier, 2005; Tarasov *et al*., 2012).

In contrast, comparatively little is known about its dynamics prior to the LGM, largely because most geological evidence on land has been erased by ice flow during the late stages (e.g. during final deglaciation). Thus, whilst ocean sediment records are particularly useful for investigating pre-LGM iceberg fluxes and meltwater events (e.g. Hesse and Khodabakhsh, 1998; Kirby and Andrews, 1999; Andrews and MacLean, 2003; Farmer *et al.*, 2003; Hesse *et al*., 2004; Rasmussen *et al*., 2003; Hemming, 2004; Stokes *et al.*, 2005), we

77   have much less data to develop and/or test both conceptual and numerical models of ice sheet

78   dynamics. Summarising a special issue of papers widely seen as a benchmark of knowledge

79   on the Laurentide Ice Sheet (LIS), Andrews noted that "we have a fair knowledge of the late

80   glacial history of the ice sheet back to about 20 ka; an imperfect knowledge of events

81   between 20 and 40 ka; and sketchy knowledge of the events that led to the development of

82   the ice sheet during marine isotope stages 5 through 4" (Andrews, 1987: p. 316).

83   Notwithstanding these limitations, impressive attempts have been made to link 'pockets' of

84   evidence in the geological record that survived modification during deglaciation (e.g. relict

85   landform and striae evidence; and till stratigraphic data) in order to reconstruct the

86   approximate ice sheet configuration at broad time intervals prior to the LGM (e.g. Fulton,

87   1984; Dredge and Thorleifson, 1987; St-Onge, 1987; Vincent and Prest, 1987; Fulton, 1989;

88   Boulton and Clark, 1990a, b; Clark and Lea, 1992, synthesised in Clark *et al.*, 1993; Kleman

89   *et al.*, 2002; Kleman *et al.*, 2010). However, the fragmentary nature of the evidence precludes

90   a robust chronology of ice sheet volume and dynamics and these reconstructions are,

91   necessarily, tentative, and lack quantified uncertainty (e.g. especially in terms of ice volume).

92   Thus, although we know that the ice complex underwent major fluctuations from the last

93   major interglaciation (Oxygen Isotope Stage: OIS 5e) to the LGM (cf. Clark *et al.*, 1993), the

94   timing of these events is poorly constrained and the ice dynamics are largely unknown. This

95   leaves several fundamental questions unanswered regarding its pre-LGM history. For

96   example: where was its inception located and how did major ice domes/divides evolve

97   through time? What was the magnitude and timing of major fluctuations in ice sheet volume;

98   and how did rates of change compare to those during deglaciation? How did the basal thermal

99   regime evolve? Where were the major ice streams located during the growth phase?

100   One way to address the above questions is through numerical ice sheet modelling, which can

101   provide a continuous evolution of ice sheets through time. With this in mind, this paper

4

102 presents the results of numerical modelling of the dynamics of the NAISC from its inception

103 through to the LGM (120 to 20 ka). We do this using a previously-published Glacial Systems

104 Model (GSM),which has been calibrated against a large and diverse set of geophysical data

105 (relating to relative sea level, marine limits, present day rates of uplift, palaeo-lake levels) for

106 the deglacial interval (e.g. Tarasov and Peltier, 2004; 2007; Tarasov *et al*., 2012). Although

107 few calibration data are available for intervals prior to the LGM (e.g. dated ice margin

108 positions), we suggest that the dynamical self-consistency of the model implies that the

109 robust deglacial calibration (see Tarasov *et al*., 2012) should increase the plausibility of the

110 modelled pre-LGM chronology. The calibration provides a probabilistic output of ice sheet

111 properties from effectively hundreds of thousands of model runs. This represents an advance

112 over the small number of previous modelling studies that simulate the pre-LGM evolution of

113 the ice complex but which have tended to lack substantial data-model calibration (e.g.

114 Tarasov and Peltier 1997a, b; Marshall *et al*., 2000; Bintanja *et al.*, 2002) and/or deal with

115 shorter time intervals (e.g. the LGM in Tarasov and Peltier, 1997a; b; 120-55 ka in Kleman *et*

116 *al*., 2002).

117 Our focus here is on determining the spatial extent and ice volume through time and the

118 associated changes in the dynamics of the ice sheet (e.g. in terms of the evolving basal

119 thermal regime, velocity, etc.). This approach is not without its limitations (which we discuss

120 below) but we believe it offers some significant insights into the pre-LGM history of the

121 NAISC and generates some important hypotheses for future work to test.

122

123

124 **2. Methods**

125   The GSM is comprised of a 3D thermo-mechanically coupled ice-sheet model with visco-

126   elastic bedrock response and a fully coupled diagnostic surface drainage solver; along with

127   various smaller modules dealing with surface mass-balance, ice calving, ice-shelves, and

128   basal drag (Tarasov and Peltier, 2004; Tarasov *et al.*, 2012). The drainage solver is fully

129   coupled in that evolving surface topography determines drainage, while pro-glacial lakes

130   from the drainage solver affect the ice sheet via lacustrine calving, mini-ice shelves, and load

131   effects on bed visco-elastic response. Drainage is recomputed every 100 years as a simple

132   downslope 'depression fill' calculation as opposed to a dynamic solution of open channel

133   hydraulic flow (Manning equation).

134   The model uses the 'shallow-ice approximation' (SIA), with a Weertman type power law (i.e.

135   basal velocity is proportional to a power of driving stress) for basal sliding (exponent 3) and

136   till-deformation (exponent 1). The thermodynamic solver for the ice is based on conservation

137   of energy, only ignoring horizontal conduction due to the scales involved. The bed thermal

138   model computes vertical heat conduction to a depth of 3 km and takes into account

139   temperature offsets at exposed ground layers due to seasonal snow cover and varying thermal

140   conductivity of thawed and frozen ground (see Tarasov and Peltier, 2007).

141   The GSM uses a 'basal flow factor' that is derived from a combination of the 'Sedmap' data-

142   set (Laske and Masters, 1997), surficial geology map of Canada (Fulton, 1995) and seismic

143   surveys from Hudson Bay (Josenhans and Zevenhuizen, 1990), see Figure 1. Of most

144   relevance is whether the value is equal to 0 or not, corresponding to whether fast flow due to

145   basal sliding and/or subglacial sediment deformation is inhibited or permitted. An important

146   caveat is that the model assumes that the sediment distribution is the same throughout the

147   studied interval, which is convenient but potentially inaccurate (although to what extent for

148   such a grid-scale has yet to be ascertained). It may be that the distribution of sediments was

149   quite different at the start of the last glacial cycle, but there are some regions (e.g. Hudson

150 Bay Lowlands) where the stratigraphic record indicates that fine-grained marine and

151 lacustrine sediments were equally abundant after the previous interglaciation (e.g. Allard *et*

152 *al*., 2012).

153 The availability of soft sediments is likely to influence the location of zones of fast flow (ice

154 streams) in the model output. Thus, the lack of detailed knowledge of pre-LGM sediment

155 distribution introduces greater uncertainty in terms of their location during ice sheet build-up.

156 However, it should also be noted that a primary control on fast flow are the basal

157 thermodynamics, which are an accurate predictive component of the model (although subject

158 to uncertainties in climate forcing); and that soft deformable sediments are not an essential

159 pre-requisite for ice streaming (cf. Stokes and Clark, 2003; Winsborrow *et al*., 2010).

160 Additionally, the parameters controlling the strength of fast flow due to sliding and/or sub-

161 glacial till-deformation are subject to calibration, which helps further reduce uncertainties.

162 The GSM is run at a 0.5° latitude by 1° longitude grid resolution and 39 calibration

163 parameters determine the climate forcing, basal velocity, ice calving, etc. Model runs are

164 initiated with no ice at 122 ka (except over the northwest tip of a stub of Greenland that falls

165 within our study region and permits glaciation of Ellesmere and Axel Heiberg Islands) and

166 results are from a high-probability subset of the calibrated model runs. Calibration involves

167 parameter vectors (each consisting of a set of values for the 39 model calibration parameters)

168 being obtained from Markov Chain Monte Carlo sampling with respect to the emulated fits to

169 observational constraints. Prior parameter ranges are given in Tarasov *et al*. (2012) but their

170 specification in such a large ensemble calibration is largely irrelevant as long as they are wide

171 enough.

172 As noted above, the calibration dataset includes little pre-LGM geological constraint.

173 Although glacial geologic data exist (e.g. multiple till stratigraphies that record multiple ice

174 sheet advances/occupations of specific regions), they are generally rather poorly dated and,

175   moreover, there are very few (if any?) dated ice margin positions, which would be of most

176   use for model calibration, as in the deglacial calibration procedure (Tarasov *et al*., 2012). The

177   calibrated set of runs from Tarasov *et al.* (2012) were therefore subject to subsequent sieving

178   (Table 1) to ensure ice volumes were within plausible ranges (taking into account the range

179   of pre-LGM values for the other major ice sheets from ongoing and past calibrations). This

180   small set of constraints alone proved significant enough to require modification of the climate

181   forcing temporal dependence. Thus, the only change from the model setup described in

182   Tarasov *et al.* (2012) is that a series of linear transformations were used to deform the

183   temporal history of the climate weighting index, see Figure 2, for interpolation between

184   present-day observed climate and LGM climate from General Circulation Climate model runs

185   (from the PMIP II database: Braconnot *et al.*, 2007). This is necessary to attain an

186   approximate phase match with the inferred sea level chronology of Waelbroeck *et al.* (2002)

187   and results in a ca. 5 ka shift at the start of the model runs (122 ka), which gradually deforms

188   to match the LGM climate (Fig. 2).

189   It should also be noted that the climate index is not simply a prescribed mass balance forcing

190   *per se*. The index is a weighting function for the interpolation between present-day observed

191   and LGM climate and there are a number of other controls and feedbacks that are subject to

192   ensemble calibration (see Tarasov *et al*., 2012). Hence, the climate forcing is calibrated

193   against data with respect to ice sheet constraints and 28 of the 39 calibration parameters

194   control climate forcing and feedbacks in the model. Orbital configurations will, of course,

195   vary over the last glacial cycle and, in particular, insolation represents a critical forcing for

196   ice sheet inception. These variations are, to some extent absorbed by the climate index (albeit

197   incompletely).

198   Ensemble means and variances presented below are generated assuming a Gaussian

199   distribution of model likelihood given model misfit to observations. The key advantage of the

200 ensemble approach is that it computes a probability distribution of past ice sheet evolution

201 with explicit treatment of uncertainties in terms of both observational constraints and

202 calibration parameters. It should be noted, however, that uncertainties due to inherent

203 limitations in the GSM and parameterised form of the climate forcing are, at best, only

204 partially quantified and so indicated uncertainty estimates below are unavoidably incomplete.

205 Drawing conclusions from only a single model run (or small set thereof) would be highly

206 speculative and so we focus here on analysis of ensemble means of a subset of 'best-fit'

207 model runs that represent the likelihood of ice sheet properties (e.g. ice thickness, basal

208 velocity) in any given location through time.

209 The model includes the entire NAISC (cf. Tarasov *et al*., 2012) for the obvious reason that all

210 components are known to have been coalescent for at least part of the last glacial cycle.

211 However, we primarily focus on the LIS (although not exclusively) because: (a) it covered a

212 much larger area than the other components and was, therefore, more significant in terms of

213 global ice volume/sea level fluctuations; (b) significantly more work has been undertaken on

214 the LIS compared to the other components (both pre- and post-LGM), such that most

215 calibration data from the deglacial interval relate to the LIS; and (c) the high relief and

216 complex topography that characterises some components (e.g. the CIS) introduces

217 considerable complexity and additional uncertainty for numerical modelling (and confidence

218 in the results is correspondingly weaker), further exacerbated by the relatively large model

219 grid cells.

220

221

222 **3. Results**

223 *3.1. Ice sheet inception following the last interglaciation*

224   The timing of inception is uncertain and is heavily dependent on the climate forcing

225   interpolation function but, in order to explore the geographical location of ice sheet growth

226   during the first few thousand years following the last interglaciation, we extracted ensemble

227   probability plots of the likelihood of ice being >1 m thick. Results are presented in Figure 3,

228   which shows substantial ice accumulation from around 118 ka, with inception mainly on

229   mountains and high plateaux of the central and eastern Canadian Arctic Archipelago (CAA)

230   and over Foxe Basin. Inception then spread rapidly southward into Hudson Bay, south-

231   westward into northern Keewatin, and westward across the remainder of the CAA. By 112

232   ka, it is probable that the ice complex covered most of northern Canada with a southern

233   margin tracing the coast of Hudson Bay and across Keewatin to Great Slave and Great Bear

234   Lake. A nearly full-bodied CIS developed over the same time interval and may have

235   coalesced with the LIS in the north-east.

236

237   *3.2. Ice sheet extent and volume*

238   Figure 4 shows snapshots of the modelled weighted ensemble average of basal velocity and

239   ice sheet geometry for each of the major Oxygen Isotope Stages (OIS) since the last

240   interglaciation (i.e. 5d, 5c, 5b, 5a, 4, 3 and 2). Figure 5 shows the corresponding ice sheet

241   volumes expressed as metres of sea level equivalent and the rate of ice volume change.

242   Following inception, our modelling shows the NAISC gradually expanded to cover most of

243   mainland Canada by OIS 5d (110 ka, Fig. 4). Note, however, that although ice covered

244   around 80% of the area that was later occupied by the larger ice sheets during OIS 4 (65 ka)

245   and OIS 2 (25 ka), the modelled ice thicknesses are much less (eustatic sea level equivalent

246   ca. 25 m compared to 80 m at the LGM: Fig. 5). Most of the OIS 5d ice sheet was cold-based

10

247   and the major ice domes/divides of the LGM configuration (e.g. Dyke and Prest, 1987) are

248   less well developed (i.e. thinner over Quebec-Labrador, Foxe Basin and Keewatin).

249   During OIS 5c (100 ka) the ice cover shrank towards the north-eastern CAA and is depicted

250   as a thin ice sheet that likely resembled a coalescence of cold-based plateau-ice fields, with

251   ice thickness typically <1000 m and with an ice dome over Foxe Basin/north-east Keewatin.

252   The ice cover thickened slightly and expanded south-westward again during OIS 5b (90 ka),

253   with the Foxe-Keewatin dome remaining the most prominent feature, but it failed to reach the

254   thickness and extent of the OIS 5d configuration at 110 ka. The transition to OIS 5a (80 ka)

255   saw the ice sheet shrink to it minimal extent since OIS 5e, with a volume of just a few metres

256   of sea level equivalent (Fig. 5) locked up in thin and mainly cold-based ice in and around the

257   early inception grounds.

258   OIS 4 (65 ka) saw a rapid expansion of ice cover from around 80 ka to 65 ka, containing an

259   additional volume equal to 60 m of sea level at the end of that 15 ka period (up to 10

260   m/thousand years: Fig. 5). The ice sheet configuration by 65 ka was almost identical to its

261   LGM counterpart (compare to 25 ka) in terms of both its extent and the location of major ice

262   divides (over Labrador, Foxe Basin/north-east Keewatin: cf. Dyke and Prest, 1987; Clark *et*

263   *al.*, 2000), but the difference here, compared to the build-up towards the LGM, is that the

264   growth phase was continuous and rapid. There then followed an equally rapid period of mass

265   loss to the start of OIS 3 (60 ka), which is mostly reflected in deglaciation of the southern

266   margin and a major reduction in ice thickness. This deglaciation at the OIS 4/3 transition saw

267   a peak sea level contribution of up to 16 cm per century (Fig. 5). Several periods of ice

268   growth and successively less significant ice shrinkage followed between 55 and 25 ka (Fig.

269   5), culminating in the LGM configuration of OIS 2 (~25 ka: cf. Clark *et al*., 2009).

270

271 *3.3. Basal thermal regime and patterns in ice sheet velocity*

272 The model calculates the evolving basal thermal regime, which strongly influences basal ice

273 velocity and the drainage patterns. As in most numerical ice sheet models, ice velocities are

274 dynamically determined based on the evolving driving stress and basal temperature of the ice,

275 and on the presence of deformable sediment. Rapid ice flow (e.g. ice streaming) can only

276 occur when the basal temperature approaches the pressure melting point.

277 Figure 6 shows a time series of the fraction of the bed occupied by warm-based ice from our

278 new ensemble and from an 'old ensemble' (Tarasov and Peltier, 2007). A largely cold-based

279 ice cover evidently evolves to a largely warm-based ice cover, as ice sheets expand and

280 thicken, in agreement with previous work (Marshall and Clark, 2002). For the first 50-60 ka

281 of glaciation, only 20-30% of the bed is warm, but this fraction increases to nearly 50% as the

282 ice complex grows during OIS 4 (ca. 65 ka). Following a reduction in the warm-based

283 fraction around 60-55 ka, it then generally increases towards the LGM (25 ka), when it is

284 >50%. The results of the 'old' versus 'new' ensemble are broadly similar, although there is

285 greater divergence for the period 55 to 30 ka. These differences in Figure 6 are likely to

286 reflect the deformation of the climate interpolation function (Fig. 1) and the additional

287 constraints and parameters in the new calibration. The comparison is presented to underline

288 the uncertainties in this and other modelling and the resultant contingent nature of the results.

289 The velocity patterns of the modelled ice complex (Figure 4) closely resemble the patterns

290 seen in modern-day ice sheets (e.g. Joughin *et al.*, 1999; Bamber *et al.*, 2000). Slow-flowing

291 (cold-based) domes feed zones of intermediate velocity that are tributaries to discrete zones

292 of rapidly-flowing ice (>500 m a^{-1}). Even the relatively small ice sheets exhibit fast flow

293 zones surrounded by cold-based ice. The relatively thin ice sheets between 100 and 80 ka, for

294 example, possess several arteries of rapidly-flowing ice, mostly restricted to marine margins

295 that flow through topographic troughs, e.g. Hudson Strait, Lancaster Sound, etc. (Fig. 4).

296　During more extensive glaciations (OIS 4 and 2), major zones of fast flow are located in the

297　same marine troughs as in the smaller ice sheets but also occupy troughs further to the SE

298　(e.g. Gulf of St Lawrence) and N/NW (e.g. Mackenzie River corridor). Broader zones of

299　enhanced flow also formed inboard of the southern terrestrial margin during periods of

300　maximal ice coverage, with tributaries extending several hundred kilometres up-ice. These

301　are particularly noticeable around the Great Lakes region and over the western prairies, some

302　in association with proglacial lakes.

303　To show the temporal variability of these fast flow zones at a higher temporal resolution,

304　Figure 7 presents time series' of basal velocity at four locations where fast flow is generated

305　by the model and where there is robust geological evidence for ice stream activity during

306　final deglaciation (see inventories in Patterson, 1998; Stokes and Clark, 2001; Winsborrow *et*

307　*al.*, 2004; Stokes and Tarasov, 2010).

308　Hudson Strait (Fig. 7a) was a major conduit of fast flow during deglaciation and a dominant

309　source of Heinrich events throughout the last glaciation (cf. MacAyeal, 1993; Andrews and

310　MacLean, 2003; Hemming, 2004). The time series of basal velocity for this location denotes

311　high velocities (>500 m a^{-1}) sustained from about 65 ka through to the LGM, but with a

312　slowing down around 55 ka and, to a lesser degree 40 ka; a pattern which broadly matches ice

313　sheet volume (Fig. 5a). Note that the near shut-down in Hudson Strait flow starting at 30 ka is

314　an imposed feature of the model to dynamically facilitate the correct timing of Heinrich

315　events 1 and 2. As detailed in Tarasov *et al.* (2012), the strength of the reduction in velocities

316　(but not the timing) is under the control of calibrated parameters (i.e. the strength was not

317　'hand-tuned'). We stress that all other streaming is under free physical control and that the

318　dynamic facilitation in Hudson Strait (between 30 and 20 ka) is the only imposed feature in

319　all model runs and is not important in the context of this paper, where much of the focus is on

320　ice sheet dynamics prior to 30 ka.

321 Located at the north-western margin of the ice sheet, the M'Clure Strait Ice Stream was

322 similar in size to Hudson Strait and has also been linked to major iceberg export events in the

323 Arctic Ocean (Stokes *et al.*, 2005; 2009). Model output indicates a similar onset and pattern

324 of velocity to Hudson Strait at 65 ka but with comparatively lower velocities (Fig. 7b). This

325 location exhibits less variability than Hudson Strait, as depicted by a narrower range of

326 uncertainties and with a mean basal velocity typically falling within 500-1000 m a^{-1} from 70-

327 20 ka, whereas Hudson Strait often exceeds 2000 m a^{-1}. A similar pattern is seen in the Gulf

328 of St Lawrence (Laurentian Channel Ice Stream: Shaw *et al.*, 2006), where rapid ice

329 velocities occur during maximal ice volumes from ca. 30 ka and with some activity from 70

330 to 65 ka (Fig. 7c).

331 For comparison to the marine-based outlets, the time series of basal velocity for the land-

332 terminating Des Moines lobe is also shown (Fig. 7d). This lobe is thought to have been the

333 outlet of a large 'terrestrial ice stream' that may have operated several times since the LGM,

334 with a prominent margin position between 30 and 20 ka, and a more recent re-advance

335 around 14 ka attributed to ice streaming (Patterson, 1997). It is clear that rapid velocities are

336 not a persistent feature but tend to only 'switch on' during glacial maxima (e.g. around 65-70

337 ka: Fig. 7d). We also note some possible cyclicity in this region from ca. 50 ka, with the

338 gradual build of streaming velocities often culminating in a sharp drop and then a further

339 steady increase.

340

341

342 **4. Discussion**

343 *4.1. Ice sheet inception and coalescence*

344   The location of North American ice sheet inception has been debated since Flint's (1943)

345   suggestion of a highland origin and windward growth for the LIS (see review in Ives *et al*.,

346   1975; Stroeven *et al*., 2002). This hypothesis has gradually been replaced by a new paradigm

347   that invokes 'instantaneous glacierisation' of Arctic and subarctic plateaux and uplands (e.g.

348   Ives, 1957; 1962; Andrews *et al*., 1976; Andrews and Barry, 1978; Andrews and Mahaffy,

349   1976; Dyke *et al*., 1989; Kleman *et al*., 2002; Wolken *et al.*, 2005, 2008). This paradigm is

350   based on the notion that these regions are close to the threshold of glaciation (cf. Williams,

351   1978a, 1979; Bromwich *et al.*, 2002), as illustrated by the fact that thin plateau ice-fields

352   spread over tens of thousands of square kilometres there during the Little Ice Age (e.g. Ives,

353   1962; Williams, 1978b). However, the precise timing of the last glacial epoch is not well

354   known and albedo and temperature lapse-rate feedbacks must have acted to amplify relatively

355   low-amplitude orbital cooling trends. In particular, global sea level lowering of at least 20 m

356   and as much as ~75 m over 10 ka (cf. Andrews and Mahaffy, 1976) suggests a rapid growth

357   that has, previously, not been easily captured by numerical models (cf. Marshall, 2002;

358   Bintanja *et al*., 2002).

359   In terms of location, our results broadly agree with previous numerical modelling (e.g.

360   Tarasov and Peltier, 1997a; Marshall, 2000; Marshall and Clarke, 1999; Marshall *et al.*, 2000;

361   Bintanja *et al*., 2002; Kleman *et al.*, 2002), that clearly support the location of inception on

362   Arctic/subarctic plateaus along the eastern seaboard, with Ellesmere Island, Axel Heiberg,

363   Devon and Baffin Islands seeding the proto-LIS/IIS within a few thousand years of the last

364   interglaciation (Fig. 3). An embryonic dome over Quebec-Labrador formed a few thousand

365   years later (cf. Vincent and Prest, 1987; Marshall *et al*., 2000; Andrews and Mahaffy, 1976).

366   It had probably been established by 114 ka, but it is certainly apparent in the modelled ice

367   sheet topography for 110 ka (Fig. 4) and supports inferences from striae and dispersal trains

368   of an early ice build-up north of the St Lawrence River in the highlands of Quebec (cf.

369 Veilette *et al.*, 1999; Veillette, 2004). A similarly early but short-lived build-up of the

370 Appalachian ice complex is also shown during OIS 5 (at 110 ka Fig. 4), which has also been

371 invoked based on till stratigraphic data (McDonald and Shilts, 1971; Lamothe *et al*., 1992;

372 Clark *et al*., 1993). The early presence of ice in Hudson Bay/Strait is also in agreement with

373 sedimentary sequences in the Hudson Bay Lowlands, where organic bearing units assumed to

374 be of the last interglaciation are often capped (or completed) by a thick sequence of

375 rhythmites, which suggest that the Hudson Bay watershed was blocked by ice, thereby

376 creating a large proglacial lake prior to the next ice advance (e.g. Skinner, 1973; Allard *et al*.

377 2012).

378 Although there are issues that hinder the modelling of the CIS at this grid resolution (see

379 section 4.2.3), it is also noteworthy that the CIS is established and probably coalescent with

380 the LIS by 112 ka. Ryder and Clague (1989) and Clark *et al*. (1993) comment that the timing

381 of the first major ice sheet development in this region during the last glacial cycle (known as

382 the 'penultimate glaciation') is uncertain (OIS 4 or 5?) but our modelling clearly supports a

383 large CIS during OIS 5.

384 A key result of our modelling is the relatively large ice sheet at 110 ka, with the LIS

385 coalescent with the CIS (Fig. 4; Fig. 5). This agrees with inferences from one of the earliest

386 numerical modelling studies, albeit using simplified physics (e.g. Andrews and Mahaffy,

387 1976), that suggested that large ice sheets can develop in about 10,000 years under certain

388 conditions. Capturing the rapid growth of North American ice to a maximum at 110 ka,

389 described as the "explosive ice sheet growth suggested by the marine record" (Marshall,

390 2002: p. 133), is a successful feature of our model and supports the assertion of Cutler *et al*.

391 (2003) that ice sheet expansion need not be inherently slow and is often characterised by

392 rapid intervals of growth. Our modelled rate of maximum sea level fall during growth of the

393 OIS 5d ice sheet (between 120 and 110 ka) approaches 5 m/1000 yr (Fig. 5), which is almost

394   identical to the figure (4.2 m/1000 yr) quoted by Andrews and Mahaffy (1976) in their

395   modelling study. Furthermore, deglaciation of the OIS 5d ice sheet led to a peak sea level

396   contribution of >5 m/1000 yr and we also note an equally rapid rise in sea level at the

397   OIS5b/5a transition, which has been identified in coral reef records (e.g. Cutler *et al*., 2003).

398   Despite their relatively large areal extent, these early ice sheets (e.g. 110 ka) were generally

399   thin and largely cold-based. This may result from more limited precipitation, but is probably

400   a reflection of the short time period over which they could grow (e.g. inception over Hudson

401   Bay only starts between 116-114 ka) and the fact that it takes time to warm-up the base of the

402   ice.

403   Following inception, our results depict ice episodically spreading from inception centres into

404   Hudson Bay for the period 120-70 ka, when ice cover alternates between a 'proto-Laurentide-

405   Innuitian' ice sheet and independent ice domes (cf. Marshall *et al*., 2000); although an ice-

406   free corridor remains open between the LIS and the CIS for the period ~105 ka to ~75 ka. As

407   noted by Marshall *et al.* (2000), this behaviour reflects both Milankovitch- and millennial-

408   frequency climate oscillations, resulting in a dynamic ice sheet with migrating domes and

409   divides (cf. Boulton and Clark, 1990a; b). Moreover, these embryonic domes acted as the

410   seed points for major dispersal centres during longer or colder stadials and probably survived

411   later inter-stadials as residual domes (cf. Kleman *et al.*, 2010).

412

413   *4.1.1 Inception over Foxe Basin?*

414   Perhaps the most unexpected aspect of our modelled inception pattern is the very early

415   nucleation of ice over Foxe Basin (ca. 118 ka: Fig. 3) and then Hudson Bay. Generally, it has

416   been assumed that these large marine basins were infilled by ice flowing from adjacent

417   domes on land, but our modelling clearly depicts ice in Foxe Basin at 118 ka before adjacent

418   land has any substantial ice cover. This might suggest that marine processes (e.g. sea ice

419   formation) can play an important role in ice sheet inception and, indeed, this is exactly what

420   Denton and Hughes (1981) proposed in their Marine Ice Transgression Hypothesis (MITH).

421   Under this scenario, climatic cooling leads to permanent sea-ice, whose albedo allows the

422   regional snowline to descend to sea level. A mechanism to expand the snowline to low

423   elevations is shared by proponents of the instantaneous glacierization hypothesis (e.g. Ives et

424   al., 1975), but the MITH also allows for the sea ice to thicken into ice shelves that eventually

425   ground in shallow marine embayments, thereby creating marine ice domes that expand into

426   ice sheets (Hughes, 1987). In his theoretical treatment, Hughes (1987) specifically cited Foxe

427   Basin as one of the first places where an ice shelf might ground in North America and then

428   spread south into Hudson Bay.

429   The importance of sea ice formation in lowering regional albedo during glacial inception was

430   also emphasised by Koerner (1980), who further noted that sea ice may have "allowed

431   survival of the [North American] ice sheet through the warmer periods of the interstadials and

432   promoted ice cap growth during ensuing periods, which might not have had the right

433   conditions to start the ice sheet core itself" (p. 157). Using a GCM, Dong and Valdes (1995)

434   also concluded that orbitally-induced changes in sea surface temperature and thus sea ice

435   were likely to be a very important in initiating glaciation in the Canadian Arctic.

436   Although Hughes (1987) acknowledged that windward growth (Flint, 1943) and

437   instantaneous glacierization (Ives, 1957) could have been important for inception patterns in

438   other northern hemisphere ice sheets, he suggested that marine ice transgression was

439   probably dominant in the Canadian Arctic Archipelago and our modelling also points towards

440   the importance of marine processes (sea ice formation) in this region (Fig. 3). However, there

441   are other factors which might also be important. These include the Sangamonian topography

442   (adjusted so that the surface topography at the end of a model run is close to that observed for

443   present-day), the degrees of freedom in the climate forcing, and perhaps the representation of

444   ice calving and ice shelves. Thus, whilst the model potentially points towards the importance

445   of marine processes in North American ice sheet inception, a more complete sensitivity

446   analysis is required to reduce uncertainties in the causal explanation. In particular, the use of

447   the SIA limits the models ability to fully capture marine ice sheet physics, which are likely to

448   have been particularly important during OIS 5, when the ice sheet margins advances and

449   retreats repeatedly over high latitude seaways (e.g. in Foxe Basin and Hudson Bay/Strait). As

450   such, this finding should be regarded as preliminary.

451

452   *4.2. Comparison to previous reconstructions of ice sheet build-up to the LGM*

453   We now compare our model results with previous attempts to reconstruct the pre-LGM

454   evolution of the NAISC and, particularly, the LIS. We refrain from a detailed comparison

455   with localised records of pre-LGM ice sheet deposits (reviewed, for example, in St-Onge,

456   1987; Vincent and Prest, 1987; Dredge and Thorleifson, 1987; Clark *et al.*, 1993), which is

457   beyond the scope of our ice sheet-wide synthesis. Instead, we focus on comparison to

458   previous reconstructions of the broad patterns of growth and decay.

459

460   *4.2.1. Comparison to previous numerical modelling studies*

461   Few studies have used numerical ice sheet models to examine the evolution of the LIS during

462   the last glacial cycle (Tarasov and Peltier, 1997a; b; Marshall, 2000; Marshall and Clarke,

463   1999; Marshall *et al.*, 2000; Marshall and Clark, 2002; Bintanja *et al.*, 2002). Typically, they

464   focused on capturing the main features of the LGM ice sheet, presented as a time series of ice

465   sheet properties (usually volume, but sometimes extent, maximum thickness, warm-based

466   fraction, etc.) from the last interglaciation (ca. 120 ka) to present (e.g. Marshall *et al.*, 2000).

467　Early attempts using a simplified energy balance model tended to depict a monotonic growth

468　towards the LGM (e.g. Tarasov and Peltier, 1997a) but more recent climate forcing

469　prescribed by the GRIP (Greenland Ice Core Project) record has resulted in most models

470　reproducing the higher-frequency growth and decay cycles (e.g. Marshall *et al*., 2000;

471　Marshall and Clark, 2002; Bintanja *et al*. 2002; Kleman *et al*., 2002), that our modelling

472　unsurprisingly replicates (Fig. 4 and 5).

473　In agreement with our results, most numerical modelling efforts (e.g. Marshall, 2000;

474　Marshall and Clarke, 1999; Marshall *et al.*, 2000; Bintanja *et al*., 2002) simulate early ice

475　sheet growth (OIS 5d?), albeit not always as rapid as in our modelling, followed by a

476　minimum ice extent in OIS 5a (80 ka). All models reproduce growth to a large OIS 4 ice

477　sheet, and most depict a minimum during OIS 3 (ca. 55 ka), followed by punctuated growth

478　towards the LGM. The major discrepancies amongst different numerical models largely

479　emerge in terms of the precise timing of the various maxima/minima, which is likely a

480　reflection of the specific treatment of the climate forcing. Indeed, the relatively rapid

481　increases/decreases in ice volume produced in our model are largely attributable to the high

482　frequency variability in the climate forcing index (Fig. 2), which percolate to varying extents

483　(depending on phasing, calibration parameters, duration, intensity) into the ice volume

484　curves. This is to be expected from a complex non-linear model which simulates the

485　interactions and feedbacks of numerous processes, but it is more difficult to determine the

486　potential contributions from different model processes/components (e.g. marine ice sheet

487　dynamics, ice streams, subglacial sediment deformation) that might further modulate or even

488　drive the rapid changes in ice volume. Elucidating those mechanisms would require a

489　rigorous sensitivity analysis which is beyond the scope of the present paper. Rather, we now

490　focus on the handful of studies that allow a rigorous assessment of our model results in

491   capturing the spatial and temporal patterns of ice sheet dynamics, especially in terms of the

492   geological evidence of ice extent within each OIS.

493

494   *4.2.2. OIS 5*

495   Based on a comprehensive review and synthesis of available stratigraphic records Clark *et al*.

496   (1993) focus on when and where the LIS and CIS first developed and on tracing their growth

497   to the LGM. In agreement with our modelling, they suggest that the LIS first developed over

498   Keewatin, Quebec and Baffin Island during OIS 5 (section 4.1), although our modelling

499   suggests other large islands in the CAA and Foxe Basin were equally important. They also

500   suggest that its encroachment into the western Canadian Arctic occurred late during stage 5

501   with a further possible advance into the St Lawrence Lowland. Their suggestion of early ice

502   over the western CAA was based largely on the interpretation of till sheets on Banks Island,

503   as well as equivalents on Melville Island and in the Tuktoyaktuk Coastlands, although these

504   deposits are now considered to date to OIS 2 (England *et al*., 2009). Nevertheless, the

505   presence of ice in the western CAA is certainly supported by our modelled ice sheet at 90 ka

506   (OIS 5b). Following OIS 5b, Clark *et al.* (1993) suggest that the ice sheet retreated from these

507   regions and they argued that the Hudson Bay Lowlands, the western Canadian Arctic, and the

508   St Lawrence Lowlands may have been ice free during stage 5a (albeit with no firm

509   chronological constraints), which broadly matches our reconstruction at 80 ka (Fig. 4).

510   Clark *et al.* (1993) do not discuss the possibility of a large (but thin) ice sheet during 5d (ca.

511   110 ka: Fig. 4) but their overall conclusion that an OIS 5 ice sheet developed to ca. 70% of its

512   (full-glacial) OIS 2 extent, followed by significant deglaciation, is exactly what our

513   modelling depicts. St-Onge (1987) reached a similar conclusion in noting that where the ice

514   sheet may have grown during OIS 5, most of the ice probably disappeared prior to major

515 growth during OIS 4. A similar sequence is shown in our modelling of the OIS 5a/4 transition

516 from ~80 to ~65 (see Fig. 4).

517 Further support for an extensive ice sheet in OIS 5 is also noted by Marshall *et al*. (2000)

518 who point out that marine oxygen isotope records (e.g. Shackleton, 1987; Lambeck and

519 Chapell, 2001) indicate rapid ice sheet growth in the early stages of glaciations and our

520 modelling would also suggest rapid growth and establishment of the CIS during OIS 5.

521 Indeed, elsewhere, Kleman *et al*. (1997) infer a similarly rapid growth of the Fennoscandian

522 Ice Sheet (FIS) following the last interglaciation. They used mapped flow patterns alongside

523 stratigraphic records and correlation to global sea level volumes and suggested that the FIS

524 reached an OIS 5 maximum ca. 110 ka (i.e. 5d, see also Lagerbäck, 1988a; b), before a

525 relatively rapid recession by 100 ka. However, whilst the LIS reached a similar extent to the

526 OIS 4 and 2 maxima, the OIS 5 FIS probably only covered approximately 50% of the LGM

527 extent (see Fig. 11 in Kleman *et al*., 1997; Lundqvist, 1992). Kleman *et al.* (1997) also

528 suggest that the FIS during OIS 5b was restricted in coverage and largely cold-based, which

529 is similar to our reconstructed ice sheet during this period (e.g. 90 ka on Fig. 4) and they also

530 highlight evidence of near-complete deglaciation during OIS 5a (e.g. Lagerbäck and

531 Robertsson, 1988), which is in contrast to the NAISC (see e.g. 80 ka on Fig. 4).

532 Boulton and Clark (1990a; b) used geological evidence to reconstruct the pre-LGM behaviour

533 of the LIS, but their study utilised the glacial lineation record and they inferred relative age

534 relationships based on cross-cutting flow-sets, in addition to correlation with previously

535 published till stratigraphic data (e.g. Andrews *et al.*, 1983). Their synthesis was focussed

536 largely on the Hudson Bay region and a key conclusion was that the major domes of the ice

537 sheet were highly mobile during the last glacial cycle, with ice divides shifting by up to

538 1,000-2,000 km. Specifically, they identified major changes in the location of the Keewatin

539 and Quebec-Labrador domes, either side of Hudson Bay, with periods of coalescence

540   separated by at least one relatively long period of ice-free conditions in the James Bay

541   Lowlands.

542   The first major period of coalescent domes illustrated by Boulton and Clark (1990a; b) is

543   shown from around 110 ka, which would correspond to our large ice sheet at this time.

544   However, whilst they, like us, favour a large OIS 5 ice sheet, our modelling shows a rapid

545   deglaciation of this large ice sheet by 100 ka, whereas Boulton and Clark (1990a; b) only

546   show it starting to recede from ca. 100 ka. The timing of Boulton and Clark's (1990a; b)

547   subsequent ice-free conditions in the Hudson Bay Lowlands is more uncertain but they depict

548   it at around 75 ka, based on a period of marine inundation suggested by Andrews *et al*.

549   (1983). Again, this is in broad agreement with our minimal ice extent from around 85 to 75

550   ka (Fig. 5). Andrews *et al.* (1983) further speculate that the southern shore of Hudson Bay

551   was inundated at ca.105 ka. Our modelling (e.g. Fig. 4) does not support this interpretation

552   for this time and suggests that if it did occur, it is more likely with our modelled

553   configuration by 100 ka.

554   Kleman *et al.* (2002) present a plausible evolution of the NAISC during inception and build-

555   up based on geological evidence and also in conjunction with numerical modelling. Their

556   study covered the time interval from 120 ka to 55 ka, with a particular emphasis on the 90-60

557   ka period, which incorporates the large ice sheet growth during OIS 4. Their modelled ice

558   sheet volume from 120 to 55 ka (see Fig. 1 in Kleman *et al*., 2002) mirrors the general pattern

559   revealed in our analysis, with generally low ice sheet volumes from 120 to ~70 ka, followed

560   by a period of major growth at the start OIS 4. They further suggest that this pattern captures

561   the fundamental patterns of the ice sheet gleaned from the limited geological evidence (in this

562   case, three relict ice flow patterns represented by till lineations, striae, and till fabric data

563   from northern Keewatin, the Interior Plains, and the Hudson Bay Lowlands). Both our and

564   their reconstruction, for example, indicate a build-up of the ice sheet during OIS 5 with two

565   stable dispersal centres ('nuclei') in the central Arctic/north-eastern Keewatin and Quebec-

566   Labrador that survived inter-stadial warming. The major difference during this period is our

567   modelled ice sheet expansion around 110 ka, whereas Kleman *et al*. (2002) depict minimal

568   ice volumes (~2-3 m of sea level equivalent) from 115-90 ka, as do Marshall and Clark

569   (2002).

570   Later work by Kleman *et al*. (2010) also inferred minimal ice volumes during stage 5 based

571   on a more comprehensive analysis of the glacial geological and geomorphological record,

572   which they integrated with previously published stratigraphical and chronological evidence.

573   Indeed, whereas we reconstruct a coalescent LIS and Cordilleran Ice Sheet at 110 ka (OIS

574   5d), Kleman *et al.* (2002; 2010) suggest this did not occur until ~64 ka (OIS 4). However,

575   Kleman *et al.* (2002) acknowledge that their early 'central Arctic ice sheet' may have

576   extended further south, which would be more in line with our reconstruction during stage 5,

577   and that of Clark *et al.* (1993). Kleman *et al.* (2010) also discuss the possibility of a large ice

578   sheet during a stadial in OIS 5 but they argue that 5d is unlikely because there was no

579   residual ice left over in southern Quebec immediately after 5e to seed such a large ice sheet.

580   Conversely, our modelling appears to show that residual ice is not an essential pre-requisite

581   for a large OIS 5d ice sheet (Fig. 3 and 4), but that marine processes (e.g. sea ice formation)

582   could have played an important role (see discussion in section 4.1).

583

584   *4.2.3. OIS 4*

585   During OIS 4, Clark *et al.* (1993) highlight several lines of evidence for a large ice complex

586   that perhaps advanced across the continental shelf in Nova Scotia and south into New

587   England. It may also be recorded in the Lake Ontario basin, and the western Arctic margin

588   may have reached a similar extent to that recorded during its maximal position in OIS 5.

589   Kleman *et al*. (2002) also note a massive increase in glaciated area at the OIS 5/4 transition.

590   A large stage 4 ice sheet is shown by our modelling (e.g. 65 ka: Fig. 4) and, remarkably, our

591   ice sheet at 65 ka is almost identical to the pre-Middle Wisconsinan maximum ice sheet

592   extent portrayed by Vincent and Prest (1987), see Figure 8a, which they outlined on the basis

593   of an extensive review of glacial geologic evidence, albeit with minimum age control. Indeed,

594   some of the evidence used to reconstruct this ice margin position has been subject to recent

595   revision based, in particular, on new dating (e.g. England *et al*., 2009); but the overall

596   conclusion of a large ice sheet is supported by our modelling, although not as extensive as the

597   OIS 2 ice sheet (cf. Clark, 1992a).

598   We note that Boulton and Clark (1990a; b) show a much smaller LIS extent during OIS 4 (ca.

599   60-70 ka). This was largely influenced by Andrews *et al*.'s (1983) assertion of ice free

600   conditions along the southern shore of Hudson Bay at ~75 ka (C. Clark, pers. comm.). In line

601   with Andrews *et al.* (1983), our modelling shows ice-free conditions in the Hudson Bay

602   Lowlands from ca 100 to around 75 ka (see Fig. 4; 5a) but followed by very rapid ice sheet

603   growth to a near LGM-position at 65 ka. Boulton and Clark (1990a; b) simply depict a much

604   slower growth from 75 ka, which helps explains the discrepancy between their much smaller

605   ice sheet at 65 ka, compared to our modelled mid-Wisconsinan maximum. We also note that

606   Kleman *et al.* (1997) appeal to an equally rapid build-up of the FIS during the climatic

607   deterioration at the start of OIS 4. However, their OIS 4 FIS remains around 50% smaller

608   than at the LGM, whereas our model of the LIS during OIS 4 is almost as large as it is at the

609   LGM. Rapid build-up of ice sheets at the OIS5/4 transition is also recorded in sea level

610   records and Cutler *et al.* (2003) estimate that sea level fell 60 m in <6 kyr (10.6 m/1000 yr),

611   which is certainly in agreement with our estimates of the rapidity of ice sheet growth at the

612   start of OIS 4 (Fig. 5).

613   Our OIS 4 ice maximum at ~65 ka is coincident with the oldest widely recognised Heinrich

614   event (H6) (cf. Kirkby and Andrews, 1999; Hemming, 2004) and Hemming (2004) notes that

615   this was a time of generally high IRD abundance, perhaps analogous to the LGM, which

616   further supports the presence of a large OIS 4 ice sheet. Indeed, Kleman *et al*. (2002) suggest

617   that the limited infilling of ice in Hudson Bay up until ~65 ka in their reconstruction might be

618   linked to the timing of the onset of Heinrich events (H6-H1; 67-64 to 15 ka: Hemming,

619   2004). They speculated that these intermittent massive iceberg discharge events could only

620   develop when a large ice sheet was attained. Related to this, Kleman *et al*. (2002) further

621   suggest that the LIS evolved from a largely cold-based to largely warm-based ice sheet, with

622   the implication being that "its dynamics during the early part of the cycle may have differed

623   fundamentally from that during the latter part" (p. 88). A similar conclusion was reached by

624   Marshall and Clark (2002) who argued that a substantial fraction (60-80%) of the ice sheet

625   was frozen to the bed for the first 75 ka of the glacial cycle. Our analysis of basal thermal

626   regime also shows a transition from a largely cold-based to a largely warm-based ice sheet,

627   with only 20 to 30% of the bed warm-based between 120 and ca. 70 ka (Fig. 6). We also note

628   that the FIS is thought to have undergone a similar transition from a thinner, cold-based ice

629   sheet to one with more extensive warm-based ice during the LGM (Kleman *et al*., 1997;

630   Lambeck *et al*., 2010). For example, Kleman *et al.* (1997) suggest that the scarcity of flow

631   traces from OIS 3 is likely to be a reflection of a frozen bed in the core area of the FIS that

632   persisted throughout much of the last glacial cycle. However, an important difference is that,

633   unlike the LIS, this core area was only partly consumed by inward transgressing warm-based

634   zones during the final decay phase (cf. Kleman *et al*., 1997). As such, a major difference

635   between the LIS and the FIS is that the latter, because of its more persistent cold-based core,

636   preserves a much richer record of pre-LGM flow traces. A corollary of this is that the FIS

637   may have been more "glaciologically stable" or the most part of its history (Kleman *et al.*,

638   1997: p. 296).

639   Our modelling also supports a large CIS during stage 4 (e.g. at 65 ka in Fig. 4) but this is

640   clearly in conflict with the long-standing view that there was a prolonged non-glacial interval

641   from ca. 60-30 ka (the Olympia/Boutellier Nonglacial Interval), when glaciation was

642   probably confined to mountain areas throughout much of OIS 3 (see reviews in Ryder and

643   Clague, 1989 and Clark *et al.*, 1993). As noted above (section 2), the complex topography of

644   the Cordillera presents a serious problem for continental-scale ice sheet modelling, which

645   necessitates large grid cells. For example, ablative valleys are not resolved sufficiently and

646   this may partly explain the persistence of ice in this region, when geological/chronological

647   constraints might suggest otherwise. In contrast, topographic variance over the LIS is much

648   lower and model results are, correspondingly, far more credible.

649

650   *4.2.4. OIS 3*

651   Clark *et al.* (1993) suggest that recession from the OIS 4 position occurred early in stage 3,

652   but that the ice sheet had likely started to re-advance again by 50 ka, e.g. in Illinois, the Lake

653   Ontario basin, and possibly in the headwaters of the ancestral Mississippi River in Minnesota

654   and Wisconsin. This rapid retreat from stage 4 and the re-advance of the southern margin is

655   compatible with our reconstruction (see Figs 4 and 5). Dredge and Thorleifson (1987) were

656   more tentative than Clark *et al.* (1993) in their reconstruction of the Middle-Wisconsinan

657   (OIS 3) ice sheet, and they highlight the difficulty of constraining the ice sheet extent based

658   on the dating of deposits of that age. Instead, they offered three hypotheses that range from a

659   minimum configuration with separate domes in Quebec, Keewatin and over Baffin Island

660   (their hypothesis 2, intended to accommodate the youngest Wisconsinan marine episode in

661   Hudson Bay proposed by Andrews *et al*., 1983) to a more maximal outline with an ice margin

662   as far south at the Great Lakes and extending north-westward to the Mackenzie River

663   corridor, covering most of the CAA (their hypothesis 1, see Fig. 8b, which is more in line

664   with Clark *et al*., 1993). They consider these working hypotheses to be tested and, in so far as

665   it is possible with our work, our modelling strongly supports a large ice complex (> 50 m

666   eustatic equivalent) from ~45 ka, which then gradually built up to the LGM, albeit punctuated

667   with successively less significant periods of retreat (Fig. 5). Nevertheless, given the major

668   fluctuations in ice sheet volume and extent during the relatively long OIS 3 (± 30 m eustatic

669   equivalent), it is not surprising that the poorly dated geological deposits could support either

670   an extensive or more minimal ice sheet (cf. Dredge and Thorleifson, 1987). Note, however,

671   that our modelling and other more recent work (e.g. Dredge and Cowan, 1989; Clark *et al*.,

672   1993; Allard *et al*., 2012) does not support ice free conditions in Hudson Bay during OIS 3.

673   Indeed, there is little evidence of marine sediments in the Hudson Bay Lowlands younger

674   than the Sangamonian (Bell Sea) (cf. Allard *et al*., 2012).

675   Kleman *et al*. (2010) also reconstruct ice sheet extent in OIS 3 and we note almost identical

676   configurations for this time period, with the southern margin extending into the Great Lakes

677   region and with major domes over Quebec-Labrador and in north-eastern Keewatin (cf. Fig

678   8c in Kleman *et al*., 2010 with our Fig. 4). Their late stage 3 depiction (Fig. 8b in Kleman *et*

679   *al*., 2010) likely represents our last interstadial position around 30 ka (Fig. 5a), which Dyke *et*

680   *al*. (2002) also suggest represents the most recent minimum ice extent prior to the LGM,

681   although based on un-calibrated radiocarbon dating.

682   It is important to note that even our smallest modelled OIS 3 ice complex in North America

683   was relatively extensive and consumed a global sea level equivalent of ca. 30 m (e.g. ca. 55

684   ka on Fig. 4 and 5a). This is in contrast to recent work on the FIS, which suggests that most

685   of Scandinavia might have been ice-free during the early and middle parts of OIS 3 (cf.

686 Helmens and Engels, 2010; Lambeck *et al*., 2010; Wohlfarth, 2010). Thus, if correct, a key

687 implication is that the NAISC accommodated most of the ice from the Northern Hemisphere

688 during OIS 3, although see the caveats above (section 4.2.3) regarding the likely over-

689 prediction of the CIS during this interval.

690

691 *4.2.5. Summary: OIS 5 to OIS 3*

692 Our numerical modelling depicts extensive ice sheets early during OIS 5 (5d) at 110 ka,

693 which retreat rapidly by 100 ka, and to a minimum Wisconsinan post-OIS 5e position by ca.

694 80 ka. Thereafter, large ice sheets in North America developed rapidly during OIS 4,

695 reaching a maximum extent at ca. 65 ka, before a rapid recession to an OIS 3 minimum ca.

696 60-55 ka. This was followed by a more gradual period of ice sheet growth punctuated by

697 episodes of successively less recession (minima at 40 and 30 ka) before a maximum LGM

698 position is attained at ca. 25 ka. This general evolution compares well with previous

699 numerical modelling (Marshall, 2000; Marshall and Clarke, 1999; Marshall *et al*., 2000;

700 Bintanja *et al*., 2002) and only differs in terms of the precise timing of maxima/minima.

701 However, some models fail to capture the rapid growth during OIS 5d, which is implied by

702 the global sea level record (Marshall, 2002), and which our model captures partly due to the

703 temporal deformation of the inferred GRIP temperature and partly because of the increased

704 number of parametric controls (Fig. 1).

705 In terms of geological evidence, our modelled output is generally consistent with previous ice

706 sheet-wide reconstructions that utilise geological evidence (most notably Vincent and Prest,

707 1987; Boulton and Clark 1990; Clark *et al*., 1993; Kleman *et al*., 2002; 2010). The only

708 major discrepancies are the uncertainties about the precise timing of the OIS 5 maximum

709 position (5d or 5b?: our results strongly favour 5d) and the lack of a large OIS 4 ice sheet in

710   Boulton and Clark (1990a; b), which differs from most other reconstructions (e.g. Vincent

711   and Prest, 1987; Clark *et al*., 1993). Thus, the consensus is that the pre-LGM ice sheet

712   exhibited rapid episodes of growth and decay in the build-up to the LGM. Retreat from the

713   stage 5d maximum and stage 4 maxima, for example, contributed >7 and >16 m of eustatic

714   sea level equivalent per thousand years, respectively. Indeed, comparisons suggest that the

715   NAISC was more persistent and, relatively, experienced much larger volumetric fluctuations

716   than the FIS, i.e. the OIS 5d and 4 maxima of the NAISC were almost as extensive as at the

717   LGM, whereas those in Fennoscandian were, perhaps, more restricted; and the FIS may have

718   almost disappeared altogether during OIS 3 (cf. Kleman *et al*., 1997; Lanbeck *et al*., 2010;

719   Wohlfarth, 2010).

720

721   *4.3. Ice sheet dynamics (ice streaming?) during ice sheet growth and decay*

722   Whilst our modelling supports previous inferences and extends our knowledge of the

723   probable pre-LGM volume and extent of the NAISC, it may also offer some more tentative

724   insight into ice sheet dynamics. One of the most dynamic features of an ice sheet are ice

725   streams, rapidly-flowing arteries that play a key role in ice sheet mass balance through their

726   ability to discharge large ice fluxes (typically several 10s km^3 per year). Observations of

727   modern-day ice streams have revealed changes in their velocity (Howat *et al*., 2007) and

728   position (Conway *et al*., 2002), highlighting their variability and heightening concern about

729   their future contribution to sea level (Shepherd and Wingham, 2007). The danger of

730   extrapolating these annual/decadal changes to draw conclusions about future ice sheet mass

731   balance is, however, widely acknowledged (Conway *et al*., 2002; Nick *et al*., 2009); and this

732   is one reason why numerous workers have extended the observational record through

733   investigation of palaeo-ice streaming over millennial time-scales (e.g. see reviews in Stokes

734   and Clark, 2001; Livingstone *et al*., 2012). An important consideration, however, is that

735   although palaeo-ice streams have been implicated in Heinrich events dating back to ~65 ka

736   (Hemming, 2004), most studies have focussed on their activity during deglaciation from the

737   LGM (e.g. Conway *et al*., 1999; Lowe and Anderson, 2002; Kehew *et al*., 2005; Shaw *et al.*,

738   2006; De Angelis and Kleman, 2007; Briner *et al*., 2009; Stokes *et al*., 2009; O'Cofaigh *et*

739   *al*., 2010; Stokes and Tarasov, 2010). Thus, an assessment of their prevalence during the

740   longer periods of ice sheet build-up would provide a useful comparison to their activity

741   during ice sheet demise: are ice streams equally active during growth phases? How long does

742   it take to initiate streaming in different settings and are ice streams located in similar

743   locations to their counterparts during deglaciation from the LGM?

744   An obvious question to ask, therefore, is whether the fast-flow features generated by the

745   model (see section 3.3 and Fig's 4 and 7) are akin to ice streams and, as such, whether they

746   might tell us something about their activity prior to the LGM (although there is no objective

747   velocity threshold for ice streaming, we define it here as grounded ice flowing >500 m/yr, i.e.

748   typical of the lower-end of streaming velocities in modern-day ice sheets). Unfortunately, the

749   use of the SIA and the relatively coarse resolution of the model preclude the ability to

750   accurately reproduce the full stress balance of ice streams (see Hindmarsh, 2011; Kirchner *et*

751   *al*., 2011). Thus, the extent to which the rapidly-flowing zones described above (Fig. 4)

752   represent ice streams is questionable. Nevertheless, they evolve freely in the model as per the

753   dynamically evolving basal temperature regime and stress balance. Moreover, Stokes and

754   Tarasov (2010) indicate that this model successfully reproduces deglacial ice streams where

755   geological evidence has been reported, despite the use of the SIA. Indeed, we note that the

756   location of the fast flow-features generated in our pre-LGM modelling nearly always

757   corresponds with the location of ice streams during deglaciation of the ice sheet, which have

758   been identified based on a wealth of geological evidence, e.g. in major marine troughs and

759   along the southern margin of the ice sheet (cf. Patterson, 1998; Stokes and Clark, 2001;

760   Winsborrow *et al.*, 2004; Stokes and Tarasov, 2010).

761   To illustrate the persistence of streaming velocities in both pre- and post-LGM settings in the

762   NAISC, Figure 9 shows the modelled basal velocity at 40 ka (OIS 3) with several major fast-

763   flow zones corresponding to hypothesised locations from final deglaciation. In most cases,

764   these patterns are likely the result of thermo-mechanical feedbacks, whereby thicker ice in

765   topographic troughs enhances basal warming, increasing velocity, further increasing

766   warming, further increasing velocity (Payne and Dongelmans, 1997). Thus, the main control

767   on the location of these fast-flowing outlets appears to simply be the presence and supply of

768   warm-based ice in association with soft sediment that floors these troughs. Rapid velocities

769   experienced at the land-terminating margins (e.g. the southern margin) can also be attributed

770   to the widespread availability of soft-sediments in these regions (cf. Clark, 1992b; 1994) that

771   facilitated rapid flow and surge-type behaviour through sub-glacial till deformation and/or

772   basal sliding (cf. Paterson, 19967; 1998), and sometimes in association with calving into

773   proglacial lakes (cf. Stokes and Clark, 2004). Similar processes have been invoked to explain

774   the location of episodic ice streams operating both pre- and post-LGM in the FIS (Houmark-

775   Nielsen, 2010).

776   Given that there is some indication that the modelled fast flow zones are not spurious but may

777   reflect the pre-LGM counterparts of post-LGM ice streams, we are reasonably confident that

778   model output is likely to reflect the broad pattern and timing of the major pre-LGM ice

779   stream activity, especially topographic ice streams, and can thus offer some preliminary

780   insight into this aspect of ice sheet dynamics. It should also be emphasised that the patterns of

781   basal velocity (e.g. Fig. 4) represent the mean of the ensemble of 'best-fit' model runs. In this

782   sense, they offer a probabilistic assessment of where rapid velocities are most likely to occur

783   and are, in effect, a smoothed history compared to individual runs (i.e. short-term spatial and

784   temporal variability is averaged out). Indeed, given the sensitivity of millennial-scale ice

785   stream oscillations to model numerics (Calov *et al.*, 2010) and likely to missing processes

786   such as basal hydrology, it is not the aim of this study to capture such behaviour.

787   The modelled ice sheet contains fast-flowing ice at all stages of growth from 110 to 20 ka

788   (Fig. 4). Thus, ice streaming is likely to have been a persistent feature in the pre-LGM ice

789   sheets, with even the smallest and thinnest of them being drained by large topographic ice

790   streams (note, for example, the Lancaster Sound Ice Stream in the very small ice complex at

791   110 ka). A more tentative conclusion is that the ice streams (*senus lato*) appear to increase in

792   velocity and become more prevalent with ice sheet build-up (Figs. 4, and 7). This is shown in

793   Figure 10a, which plots the total 'ice stream' flux at the margin of the grounded ice sheet

794   through time. The ice stream flux is relatively low from 115-70 ka but there is a notable peak

795   around 65 ka (OIS 4). Thereafter, the flux drops before another peak around 45 ka, followed

796   by a variable but significant increase towards the LGM. This pattern is mirrored by the

797   relative area of the ice sheet occupied by 'streaming' cells, see Fig. 10b, showing that they

798   occupy a greater proportion of the ice sheet through time, as a result of enlargement of

799   existing fast flow zones and new zones emerging.

800   We suggest that the increase in streaming activity during and following OIS 4 (Fig. 10a) is

801   due to the fact that smaller ice sheets prior to this were generally restricted to harder

802   crystalline substrates, whereas their expansion on to softer substrates and into greater contact

803   with the oceans led to unstable behaviour and an increased activity of ice streams (cf. Clark,

804   1992b; 1994; Winsborrow *et al.*, 2010). Larger ice sheets have also had more time to develop

805   a larger fraction of warm based ice (Fig. 6). It is most instructive, however, to consider the

806   total ice stream flux as a fraction of ice sheet volume. Figure 11a shows this and indicates

807   that ice stream flux at the margin exhibits strong high-frequency variation superimposed on a

808   fairly steady increase towards LGM. As one would expect, individual runs display more

809   variance than the ensemble mean, but ice streaming appears to be scaled (non-linearly) to ice

810   sheet volume. This is clear from Figure 11b, which reveals that an excess of stream flux

811   during decay, as compared to growth, is only discernible for ice volumes above 55 m eustatic

812   equivalent and grows with ice volume.

813   In summary, this is one of the first studies to assess the pan-ice sheet behaviour of ice streams

814   prior to the LGM and we view it as necessarily exploratory. However, it suggests that ice

815   streaming appears to be non-linearly scaled to ice sheet volume with a power between two

816   and three, with only moderate dependence on whether the ice-sheet is growing or decaying

817   (Fig. 11). This implies that ice streams are significant throughout both growth and decay and,

818   despite millennial scale variability, an evolving population deliver a relatively stable

819   contribution to overall ice discharge over long (>5-10 ka) time-scales (Fig. 11a).

820

821   *4.4. Future Work*

822   The results of our numerical modelling match well with previous attempts to reconstruct the

823   pre-LGM inception and build-up of the NAISC and have generated some important new

824   insights regarding its extent, volume, and dynamics. However, we identify five areas where

825   further research would benefit/complement future modelling efforts:

826   *(1)* Whilst it is reasonable to assume that ice streaming was a persistent feature of the pre-

827   LGM LIS, a potentially novel outcome of our analysis is the hypothesis that ice stream

828   activity is largely scaled to ice sheet volume. This represents an important context for our

829   understanding of ice streaming and ice sheet dynamics at timescales >10 ka and we suggest

830   that testing this hypothesis should be prioritised in future modelling that incorporates higher

831   order physics.

832   (*2*) A key uncertainty that prevents a more rigorous comparison is that there are few dates to

833   constrain the geological evidence. As noted by Clark *et al*. (1993) our knowledge of the

834   chronology of the LIS is mostly reliant on radiocarbon dating applied to the deglacial

835   interval. However, it is possible to date/bracket deposits using other methods (e.g. U-Th,

836   Ar/Ar) to bracket the extensive till stratigraphies in some areas and we note the importance of

837   recent work in the Hudson Bay Lowlands in this regard (Allard *et al*., 2012). Such constraints

838   on pre-LGM ice margin positions would thereby permit a more rigorous model calibration,

839   such as has been applied to the deglacial interval (e.g. Tarasov *et al*., 2012), especially early

840   (e.g. OIS 5 and 4) ice margin indicators (cf. Stroeven *et al*., 2002).

841   *(3)* The results of our numerical modelling complement efforts that scrutinise pre-LGM

842   iceberg-rafted debris (IRD) records in ocean sediment records (e.g. Farmer *et al.*, 2003;

843   Hemming, 2004; Roy *et al*., 2009). Our analysis highlights the importance of marine troughs

844   as locations for large palaeo-ice streams (Fig. 7) but relatively few IRD records have been

845   linked to specific ice stream catchments, although this is certainly possible through analysis

846   of their provenance (see Hemming, 2004; Andrews and MacLean, 2003; Stokes *et al*., 2005).

847   For example, Farmer *et al*. (2003) showed that the provenance of H3 is more closely

848   associated with a south-eastern (St Lawrence estuary) outlet, as opposed to Hudson Strait,

849   and we note a sharp increase in velocities of the Gulf of St Lawrence ice stream coincident

850   with H3 at around 30 ka (see Fig. 7c). Thus, there is huge potential to test and compare model

851   predictions against IRD records. Moreover, Hemming (2004) notes that there are few

852   published data on IRD events prior to H6 (~60 ka) and she highlights this as a priority for

853   future research (e.g. Roy *et al*., 2009). She draws attention, for example, to a study by

854   Rasmussen *et al*. (2003) that identified 12 IRD peaks in a sediment core off Newfoundland

855   throughout the last 130 ka whose provenance is uncertain. Results of our numerical

856   modelling of several ice stream catchments suggests that ice occupied major marine troughs

857   before 60 ka (e.g. at 110 ka and 65 ka) and, as such, could have delivered IRD to the ocean

858   sediment record. The large ice sheet at 110 ka (Fig. 4a), for example, clearly depicts ice

859   streams occupying several major marine troughs (e.g. Hudson Strait, M'Clure Strait,

860   Amundsen Gulf) and their presence and activity could be confirmed in IRD records.

861   *(4)* As noted above (e.g. with respect to the 'old' and 'new' ensemble results of the warm-

862   based fracrion: Fig. 6), the model results are heavily influenced by the climate forcing. An

863   obvious deficiency, therefore, is the uncertainty of the timing/phasing of climate evolution

864   (along with possible regional asynchroneities), which is poorly known the further back in

865   time the modelling extends. Reducing and better capturing the uncertainty of past climate

866   forcing is a non-trivial task but would clearly benefit pre-LGM ice sheet modelling.

867   *(5)* Finally, better constraints on the pre-LGM ice volume chronology are needed. On-going

868   calibration of all major ice sheets should better quantify bounds on pre-LGM partitioning of

869   sea-level contributions. But there is correspondingly an urgent need for improving the far-

870   field record of sea level change to further constrain this partitioning.

871

872

873   **5. Conclusions**

874   This paper presents a new analysis of the evolution and dynamics of the North American Ice

875   Sheet Complex during its inception and build-up to the LGM using a 3D thermo-mechanical

876   Glacial Systems Model that has undergone extensive calibration against a large and diverse

877   set of geophysical data for the deglacial interval. A probabilistic assessment of ice sheet

878   properties (thickness, basal velocity, etc) reveals major (sometimes abrupt) fluctuations in ice

879   volume ($\pm$ 10s m of eustatic sea level equivalent in <5 ka) and a highly dynamic ice complex

880   with major shifts in the location of ice divides. These rapid episodes of both growth and

881   decay are consistent with the sea level records (e.g. Cutler *et al.*, 2003).

882   In agreement with previous work, the model reproduces ice sheet inception in

883   Arctic/subarctic plateaux/uplands with ice masses growing and coalescing with a Quebec-

884   Labrador dome within <10 ka after the last interglaciation. Preliminary findings also

885   highlight the possibility of early inception over shallow marine basins, e.g. Foxe Basin (cf.

886   Hughes, 1987). Thereafter, our numerical modelling broadly matches geological evidence

887   (e.g. Kleman *et al.*, 2002; 2010; Clark *et al.*, 1993) and previous modelling attempts (e.g.

888   Kleman *et al.*, 2002; Marshall and Clark, 2002) of the evolution of the ice complex,

889   supporting the notion of a large but thin OIS stage 5d (110 ka) ice sheet that covered 70-80%

890   of the area occupied by subsequent full glacial ice sheets in OIS 4 and 2 (cf. Clark *et al.*,

891   1993). The ice complex then retreated to a small, thin OIS 5 minimum (~80 ka) over the

892   original inception grounds in north-eastern Canada, before a rapid period of growth saw a

893   large OIS 4 ice complex at ~65 ka, which largely resembled the OIS 2 (LGM) ice complex,

894   but with ~10 m less volume (eustatic equivalent). Subsequently, ice retreated rapidly to a

895   minimum OIS 3 position ~60 ka, with a peak contribution to sea level >16 cm per century.

896   The remainder of OIS 3 was characterised by several periods of growth and increasingly less

897   significant retreat, culminating in the LGM (OIS 2) ice complex.

898   Consistent with previous work (e.g. Marshall and Clark, 2002), the fraction of the bed

899   occupied by warm-based ice increases from 20-30% to >50% at the LGM, largely modulated

900   by patterns in ice volume. However, even relatively small and largely cold-based ice sheets

901   were drained by fast flow features (usually in major marine troughs). Despite limitations

902   imposed by the use of the 'shallow-ice approximation' it is reasonable to conclude that ice

903   streaming was a persistent feature during ice sheet build-up and most fast-flow features

904   generated in pre-LGM ice sheets correspond to post-LGM ice stream locations (cf. Patterson,

905   1998; Winsborrow *et al*., 2004; Stokes and Tarasov, 2010). The extent of the marine margin

906   is an important control on ice stream activity (cf. Winsborrow *et al*., 2010) and, where ice

907   exists in deep topographic troughs, ice streaming generally persists (though not necessarily

908   continuously), irrespective of climate forcing. Land-terminating ice streams appear more akin

909   to ephemeral surge behaviour over soft sediments and only occur when climate drives the ice

910   sheet margin over such sediments (e.g. at the southern margin).

911   Taken together, a potentially novel insight from our analysis is the hypothesis that the overall

912   area and flux of streams (cells >500 m a^{-1}) is non-linearly proportional to ice sheet volume.

913   This may be an artefact of our model physics and ice sheet mass balance but, if correct, the

914   implication is that ice streams are significant during phases of both growth and decay and,

915   overall, make a relatively stable contribution to mass loss, irrespective of whether the ice

916   sheet is growing or shrinking. This, in turn, has implications for the behaviour of ice streams

917   in modern-day ice sheets, where notable changes have recently been reported in their velocity

918   and thickness (cf. Howat *et al*., 2007), but which lack a long-term context. We therefore

919   suggest that further testing of this hypothesis should be a priority with a more rigorous

920   treatment of ice streaming using higher-order physics with full inclusion of

921   longitudinal/membrane stresses (cf. Hindmarsh, 2011; Kirchner *et al*., 2011). Future

922   numerical modelling would also benefit from additional geological constraint data from the

923   pre-LGM interval, such as the ongoing dating of till stratigraphies (e.g. Allard *et al.* 2012)

924   and margin positions.

925

926

927   **Acknowledgements:**

935

936   **References:**

937   Allard, G., Roy, M., Ghaleb, B., Richard, P.J.H., Larouche, A.C., Veillette, J.J. and Parent,

938   M., 2012. Constraining the age of the last interglacial-glacial transition in the Hudson

939   Bay lowlands (Canada) using U-Th dating of buried wood. *Quaternary*

940   *Geochronology*, 7 (1), 37-47.

941   Andrews, J.T., 1987. The Laurentide Ice Sheet: research problems. *Géographie physique et*

942   *Quaternaire*, 41 (2), 315-318.

943   Andrews, J.T. and Mahaffy, M.A.W., 1976 Growth rate of the Laurentide Ice Sheet and sea

944   level lowering (with emphasis on the 115,000 BP sea level low). *Quaternary*

945   *Research*, 6, 167-183.

946   Andrews, J.T. and Barry, R.G., 1978. Glacial inception and disintegration during the last

947   glaciations. *Annual Review of Earth and Planetary Sciences*, 6, 205-228.

948   Andrews, J.T. and MacLean, B., 2003. Hudson Strait ice streams: a review of stratigraphy,

949   chronology and links with North Atlantic Heinrich events. *Boreas*, 32, 4-17.

950   Andrews, J.T., Davis, P.T. and Wright, C., 1976. Little Ice Age permanent snow cover in the

951   eastern Canadian Arctic: extent mapped from Landsat 1 imagery. *Geografiska*

952   *Annaler*, 58A, 71-81.

953 Andrews, J.T., Shilts, W.W. and Miller, G.H., 1983. Multiple deglaciations of the Hudson
954   Bay Lowlands, Canada, since deposition of the Missinaibi (Last-Interglacial?)
955   Formation. *Quaternary Research*, 19, 18-37.

956 Bamber, J.L., Vaughan, D.G. and Joughin, I., 2000. Widespread complex flow in the interior
957   of the Antarctic Ice Sheet. *Science*, 287 (5456), 1248-1250.

958 Beget, J., 1987. Low profile of the northwest Laurentide Ice Sheet. Arctic and Alpine
959   Research, 19 (1), 81-88.

960 Bintanja, R., van de Wal, R.S.W. and Oerlemans, J., 2002. Global ice volume variations
961   through the last glacial cycle simulated by a 3-D ice-dynamical model. Q*uaternary*
962   *International*, 95-6, 11-23.

963 Boulton, G.S. and Clark, C.D., 1990a. A highly mobile Laurentide Ice Sheet revealed by
964   satellite images of glacial lineations. *Nature*, 346, 813-817.

965 Boulton, G.S. and Clark, C.D., 1990b The Laurentide Ice Sheet through the last glacial cycle
966   – the topology of drift lineations as a key to the dynamic behaviour of former ice
967   sheets. *Transactions of the Royal Society of Edinburgh – Earth Sciences*, 81, 327-347.

968 Braconnot, P., B. Otto-Bliesner, S. Harrison, S. Joussaume, J.-Y. Peterschmitt, A. Abe-Ouchi,
969   M. Crucifix, E. Driesschaert, T. Fichefet, C. D. Hewitt, M. Kageyama, A. Kitoh, A.
970   Lan, M.-F. Loutre, O. Marti, U. Merkel, G. Ramstein, P. Valdes, S. L.Weber, Y. Yu,
971   and Y. Zhao, 2007. Results of PMIP2 coupled simulations of the mid-Holocene and
972   last glacial maximum - part 1: experiments and large-scale features, *Climate of the*
973   *Past*, *3* (2), 261–277.

974 Bromwich, D.H., Toracinta, E.R. and Want, S-H., 2002. Meteorological perspecticve on the
975   initiation of the Laurentide Ice Sheet. *Quaternary International*, 95-96, 113-124.

976 Briner, J.P., Bini, A.C. and Anderson, R.S., 2009. Rapid early Holocene retreat of a

977   Laurentide outlet glacier through an Arctic fjord. *Nature Geoscience*, 2 (7), 496-499.

978 Calov, R., Greve, R., Abe-Ouchi, A., Bueler, E., Huybrechts, P., Johnson, J.V., Pattyn, F.,

979   Pollard, D., Ritz, C., Saito, F. and Tarasov, L., 2010. Results from the Ice-Sheet

980   Model Intercomparison Project-Heinrich Event INtercOmparison (ISMIP HEINO).

981   *Journal of Glaciology*, 56 (197), 371-383.

982 Clark, C.D., Knight, J.K. and Gray, J.T., 2000. Geomorphological reconstruction of the

983   Labrador Sector of the Laurentide Ice Sheet. *Quaternary Science Reviews*, 19, 1343-

984   1366.

985 Clark, P.U., 1992a. The last interglacial-glacial transition in North America: Introduction. In,

986   Clark, P.U. and Lea, P.D. (Eds) *The last interglacial-glacial transition in North*

987   *America: Geological Society of America Special Paper* 270, p. 269-278.

988 Clark, P.U., 1992b. Surface form of the southern Laurentide Ice Sheet and its implications to

989   ice sheet dynamics. *Geological Society of America, Bulletin*, 104, 595-605.

990 Clark, P.U., 1994. Unstable behaviour of the Laurentide Ice Sheet over deforming sediment

991   and its implications for climate change. *Quaternary Research*, 41, 19-25.

992 Clark, P.U. and Lea, P.D. (eds) 1992. The last interglacial-glacial transition in North

993   America. *Geological Society of America, Special Paper* 270, 307 pp.

994 Clark, P.U., Clague, J.J., Currey, B.B, Dreimanis, A., Hicock, S.R., Miller, G.H., Berger,

995   G.W., Eyles, N., Lamothe, M., Miller, B.B., Mott, R.J., Oldale, R.N., Stea, R.R.,

996   Szabo, J.P., Thorleifson, L.H. and Vincent, J-S., 1993. Initiation and development of

997   the Laurentide and Cordilleran ice sheets following the last interglaciation.

998   *Quaternary Science Reviews,* 12 (2), 79-114.

999   Clark. P.U., Dyke, A.S., Shakun, J.D., Carlson, A.E., Clark, J., Wolfarth, B., Mitrovica, J.X.,

1000   Hostetler, S.W., McCabe, A.M., 2009. The Last Glacial Maximum. *Science*, 325

1001   (5941), 710-714.

1002   Conway, H., Hall, B.L., Denton, G.H., Gades, A.M. and Waddington, E.E., 1999. Past and

1003   future grounding-line retreat of the West Antarctic Ice Sheet. *Science*, 286 (5438),

1004   280-283.

1005   Conway, H., Catania, G., Raymond, C., Gades, A., Scambos, T. and Engelhardt, H., 2002.

1006   Switch of flow direction in an Antarctic ice stream. *Nature*, 419 (6906), 465-467.

1007   Cutler, K.B., Edwards, R.L., Taylor, F.W., Cheng, H., Adkins, J., Gallup, C.D., Cutler, P.M.,

1008   Burr, G.S. and Bloomo, A.L., 2003. Rapid sea-level fall and deep-ocean temperature

1009   change since the last interglacial period. *Earth and Planetary Science Letters*, 206,

1010   253-271.

1011   De Angelis, H. and Kleman, J., 2007. Palaeo-ice streams in the Foxe/Baffin sector of the

1012   Laurentide Ice Sheet. *Quaternary Science Reviews*, 26 (9-10), 1313-1331.

1013   Denton G.H. and Hughes, T.J., 1980. The Arctic Ice Sheet: an outrageous hypothesis. In,

1014   Denton G.H. and Hughes, T.J. (Eds) *The Last Great Ice Sheets*. Wiley-Interscience,

1015   New York, 437-467.

1016   Dong, B. and Valdes, P.J., 1995. Sensitivity studies of Northern Hemisphere glaciation using

1017   an atmospheric general circulation model. *Journal of Climate*, 8 (10), 2471-2496.

1018   Dredge, L.A. and Thorleifson, L.H., 1987. The Middle Wisconsinan history of the Laurentide

1019   Ice Sheet. *Géographie physique et Quaternaire*, 41 (2), 215-235.

1020   Dredge, L.A. and Cowan, W.R., 1989. Quaternary geology of the south-western Canadian

1021   Shield. In, Fulton, R.J. (Ed) *Quaternary Geology of Canada and Greenland*.

1022   Geological Survey of Canada, Geology of Canada, no. 1, 214-235.

1023   Dyke, A.S., 2004. An outline of North American deglaciation with emphasis on central and

1024   northern Canada. In, Ehlers, J. and Gibbard, P.L. (Eds) *Quaternary Glaciations –*

1025   *Extent and Chronology, Part II: North America*. Developments in Quaternary

1026   Science, 2, 373-424.

1027   Dyke, A.S. and Prest, K., 1987. Late Wisconsin and Holocene history of the Laurentide Ice

1028   Sheet. *Géographie physique et Quaternaire*, 41 (2), 237-263.

1029   Dyke, A.S and Morris, T.F., 1988. Canadian Landform Examples, 7. Drumlin fields,

1030   dispersal trains, and ice streams in Arctic Canada. *Canadian Geographer*, 32 (1), 86-

1031   90.

1032   Dyke, A.S., Vincent, J-S., Andrews, J.T., Dredge, L.A. and Cowen, W.R., 1989. The

1033   Laurentide Ice Sheet and an introduction to the Quaternary geology of the Canadian

1034   Shield. In, Fulton, R.J. (Ed.) *Quaternary Geology of Canada and Greenland*.

1035   Geological Survey of Canada, Geology of Canada, no. 1, p. 178-189.

1036   Dyke, A.S., Andrews, J.T., Clark, P.U., England, J.H., Miller, G.H., Shaw, J., Veillette, J.J.,

1037   2002. The Laurentide and Innuitian ice sheets during the Last Glacial Maximum.

1038   *Quaternary Science Reviews*, 21, 9-31.

1039   Dyke, A.S., Moore, A. and Robertson, L., 2003. *Deglaciation of North America*. Geological

1040   Survey of Canada, Open File 1574.

1041   England, J., Atkinson, N., Badnarski, J., Dyke, A.S., Hodgson, D.A. and O'Cofaigh, C.

1042   (2006) The Innuitian Ice Sheet: configuration, dynamics and chronology. *Quaternary*

1043   *Science Reviews*, 25 (7-8), 689-703.

1044   England, J.H., Furze, M.F.A., Doupe, J.P., 2009. Revision of the NW Laurentide Ice Sheet:

1045   implications for paleoclimate, the northwest extremity of Beringia, and Arctic Ocean

1046   sedimentation. *Quaternary Science Reviews*, 28 (17-18), 1573-1596.

1047   Farmer, G.L., Barber, D. and Andrews, J., 2003. Provenance of Late Quaternary ice-proximal

1048   sediments in the North Atlantic: Nd Sr and Pb isotopic evidence. *Earth and Planetary*

1049   *Science Letters*, 209 (1-2), 227-243.

1050   Flint, R.F., 1943. Growth of North American Ice Sheet during the Wisconsin age. *Bulletin of*

1051   *the Geological Society of America*, 54 (3), 325-362.

1052   Fulton, R.J., 1984. *Quaternary Stratigraphy of Canada – A Canadian contribution to IGCP*

1053   *Project 24*. Geological Survey of Canada Paper 84-10, 210 pp.

1054   Fulton, R.J., 1989. *Quaternary Geology of Canada and Greenland*. Geological Survey of

1055   Canada, Geology of Canada, no. 1, 839 pp.

1056   Fulton, R.J., 1995. *Surficial materials of Canada*. Geological Survey of Canada, Map 1880A,

1057   scale 1:5,000,000.

1058   Fulton, R.J. and Prest, V.K., 1987. The Laurentide Ice Sheet and its significance. *Géographie*

1059   *physique et Quaternaire*, 41 (2), 181-186.

1060   Hemming, S.R., 2004. Massive late pleistocene detritus layers of the North Atlantic and their

1061   global climate imprint. *Reviews of Geophysics*, 42, RG1005.

1062   Hindmarsh, R.C.A., 2011. Ill-posedness of the shallow-ice approximation when modelling

1063   thermo-viscous instabilities. *Journal of Glaciology*, 57 (206), 1177-1178.

1064   Helmens, K.F. and Engels, S., 2010. Ice-free conditions in eastern Fennoscandia during early

1065   Marine Isotope Stage 3: lacustrine records. *Boreas*, 39 (2), 399-409.

1066   Hesse, R. and Khodabakhsh, S., 1998. Depositional facies of late Pleistocene Heinrich events

1067   in the Labrador Sea. *Geology*, 26 (2), 103-106.

1068 Hesse, R., Rashid, H. and Khodabakhsh, S., 2004. Fine-grained sediment lofting from
1069   meltwater-generated turbidity currents during Heinrich events. *Geology*, 32 (5), 449-
1070   452.

1071 Houmark-Nielsen, M., 2010. Extent, age and dynamics of Marine Isotope Stage 3 glaciations
1072   in the southwestern Baltic Basin. *Boreas*, 39 (2), 343-359.

1073 Howat, I.M., Joughin, I. and Scambos, T.A., 2007. Rapid changes in ice discharge from
1074   Greenland outlet glaciers. *Science*, 315 (5818), 1559-1561.

1075 Hughes, T.J., 1987. The Marine Ice Trangression Hypothesis. *Geografiska Annaler, Series A*,
1076   69 (2), 237-250.

1077 Ives, J.D., 1957. Glaciation of the Torngat Mountains, northern Labrador. *Arctic*, 10, 67-87.

1078 Ives, J.D., 1962. Indications of recent extensive glacierization in north-central Baffin Island,
1079   N.W.T., Canada. *Journal of Glaciology*, 4, 197-206.

1080 Ives, J.D., Andrews, J.T., Barry, R.G., 1975. Growth and decay of the Laurentide Ice Sheet
1081   and comparisons with Fenno-Scandinavia. *Die Naturwissenschaften*, 62, 118-125.

1082 Josenhans, H.W. and Zevenhuizen, J., 1990. Dynamics of the Laurentide Ice Sheet in Hudson
1083   Bay, Canada. *Marine Geology*, 92, 1-26.

1084 Joughin, I., Gray, L., Bindschadler, R., Price, S., Morse, D., Hulbe, C., Mattar, K. and
1085   Werner, C., 1999. Tributaries of West Antarctic Ice streams revealed by RADARSAT
1086   interferometry. *Science*, 286 (5438), 283-286.

1087 Kehew, A.E., Beukema, S.P., Bird, B.C. and Kozlowski, A.L., 2005. Fast flow of the Lake
1088   Michigan Lobe: evidence from sediment-landform assemblages in southwestern
1089   Michigan, USA. *Quaternary Science Reviews*, 24 (22), 2335-2353.

1090   Kirby, M.E. and Andrews, J.T., 1999. Mid-Wisconsinan Laurentide Ice Sheet growth and

1091   decay: implications for Heinrich events 3 and 4. *Paleoceanography*, 14 (2), 211-223.

1092   Kirchner, N., Hutter, K., Jakobsoon, M. and Gyllencreutz, R., 2011. Capabilities and

1093   limitations of numerical ice sheet models: a discussion for Earth-Scientists and

1094   modelers. *Quaternary Science Reviews*, 30, 3691-3704.

1095   Klassen, R.A. and Fisher, D.A., 1988. Basal flow conditions at the northeastern margin of the

1096   Laurentide Ice Sheet, Lancaster Sound. *Canadian Journal of Earth Sciences*, 25,

1097   1740-1750.

1098   Kleman, J. and Hättestrand, C., 1999. Frozen-bed Fennoscandian and Laurentide ice sheets

1099   during the Last Glacial Maximum. *Nature*, 402, 63-66.

1100   Kleman, J. and Glasser, N.F., 2007. The subglacial thermal organisation (STO) of ice sheets.

1101   *Quaternary Science Reviews*, 26 (5-6), 585-597.

1102   Kleman, J., Hättestrand, C., Borgström, I. and Stroeven, A., 1997. Fennoscandian

1103   palaeoglaciology reconstructed using a glacial geological inversion model. *Journal of

1104   Glaciology*, 43 (144), 283-299.

1105   Kleman, J., Fastook, J. and Stroeven A., 2002. Geologically and geomorphologically

1106   constrained numerical model of Laurentide Ice Sheet inception and build-up.

1107   *Quaternary International,* 95-6, 87-98.

1108   Kleman, J., Jansson, K., De Angelis, H., Stroeven, A.P., Hattestrand, C., Alm, G. and

1109   Glasser, N.F., 2010. North American Ice Sheet build-up during the last glacial cycle,

1110   115-21 kyr, *Quaternary Science Reviews*, 29, 17-18.

1111   Koerner, R.M., 1980. Instantaneous glacierization, the rate of albedo change, and feedback

1112   effects at the beginning of an Ice Age. *Quaternary Research*, 13, 153-159.

1113   Lagerbäck, R., 1988a. Periglacial phenomena in the wooded areas of northern Sweden –

1114   relicts from the Tärendö insterstadial. *Boreas*, 17 (4), 487-499.

1115   Lagerbäck, R., 1988b. The Veiki moraines in northerm Sweden - widespread evidence of an

1116   Early Weichselian deglaciation. *Boreas*, 17 (4), 469-486.

1117   Lagerbäck, R. and Robertsson, A.-M., 1988. Kettle holes – stratigraphical archives for

1118   Weichselian geology and palaeoenvironment in northernmost Sweden. *Boreas*, 17 (4),

1119   439-468.

1120   Lambeck, K. and Chappell, J., 2001. Sea level change through the last glacial cycle. *Science*,

1121   292, 679-686.

1122   Lambeck, K., Purcell, A., Zhao, J. and Svensson, N-O., 2010. The Scandinavian Ice Sheet:

1123   from MIS 4 to the end of the Last Glacial Maximum. *Boreas*, 39 (2), 410-435.

1124   Lamothe, M., Parent, M. and Shilts, W.W., 1992. Sangamonian and early Wisconsin events

1125   in the St. Lawrence Lowland and Appalachians of southern Quebec, Canada. In,

1126   Clark, P.U. and Lea, P.D. (Eds) The last interglacial-glacial transition in North

1127   America. *Geological Society of America Special Paper,* 270, 171-184.

1128   Laske, G. and Masters, G., 1997. A global map of sediment thickness. *EOS, Transasctions of*

1129   *the American Geophysical Union*, 78, p. 483.

1130   Livingstone, S.J., O'Cofaigh, C.O., Stokes, C.R., Hillenbrand, C-D., Vieli, A. and Jamieson, S.R.m

1131   2012. Antarctic palaeo-ice streams. *Earth-Science Reviews*, 111, 90-128.

1132   Lowe, A., and Anderson, J., 2002. Reconstruction of the West Antarctic Ice Sheet in Pine

1133   Island Bay during the last glacial maximum and its subsequent retreat history.

1134   *Quaternary Science Reviews*, 21 (16-17), 1879-1897.

1135   Lundqvist, J., 1992. Glacial stratigraphy in Sweden. *Geological Survey of Finland Special*
1136   *Paper*, 15, 43-59.

1137   MacAyeal, D.R., 1993. Binge-purge oscillations of the Laurentide Ice Sheet as a cause of the
1138   North Atlantic's Heinrich events. *Paleoceanography*, 8, 775-784.

1139   Marshall, S.J., 2002. Modelled nucleation centres of the Pleistocene ice sheets from an ice
1140   sheet model with subgrid parameterizations. *Quaternary International*, 95-96, 125-
1141   137.

1142   Marshall, S.J. and Clarke, G.K.C., 1999. Ice sheet inception: subgrid hypsometric
1143   parameterization of mass balance in an ice sheet model. *Climate Dynamics*, 15, 533-
1144   550.

1145   Marshall, S.J. and Clark, P.U., 2002. Basal temperature evolution of North American ice
1146   sheets and implications for the 100-kyr cycle. *Geophysical Research Letters*, 29 (4),
1147   2214.

1148   Marshall, S.J., Tarasov, L., Clarke, G.K.C. and Peltier, W.R., 2000. Glaciological
1149   reconstruction of the Laurentide Ice Sheet: physical processes and modelling
1150   challenges. *Canadian Journal of Earth Sciences*, 37 (5), 769-793.

1151   McDonald, B.C. and Shilts, W.W., 1971. Quaternary stratigraphy and events in Southeastern
1152   Quebec. *Geological Society of America Bulletin*, 82 (3), 683-698.

1153   Nick, F.M., Vieli, A., Howat, I.M. and Joughin, I., 2009. Large-scale changes in Greenland
1154   outlet glacier dynamic triggered at the terminus. *Nature Geoscience,* 2 (2), 110-114.

1155   NGRIP dating group, 2006. *Greenland ice core chronology 2005 (gicc05)*. IGBP
1156   PAGES/World Data Center for Paleoclimatology, Data Contribution Series # 2006-
1157   118.

1158   O'Cofaigh, C.O., Evans, D.J.A., Smith, I.R., 2010. Large-scale reorganisation and

1159   sedimentation of terrestrial ice streams during Late Wisconsinan Laurentide Ice Sheet

1160   deglaciation. *Geological Society of America, Bulletin*, 122 (5-6), 743-756.

1161   Patterson, C.J., 1997. Southern Laurentide ice lobes were created by ice streams: Des Moines

1162   lobe in Minnesota, USA. *Sedimentary Geology*, 111, 249-261.

1163   Patterson, C., 1998. Laurentide glacial landscapes: The role of ice streams. *Geology*, *26* (7),

1164   643–646.

1165   Payne, A.J. and Dongelmans, P.W., 1997. Self-organization in the thermomechanical flow of

1166   ice sheets. *Journal of Geophysical Research*, 102 (B6), 12,219-12,234.

1167   Rasmussen, T.L., Oppo, D.W., Thomsen, E. and Lehman, S.J., 2003. Deep sea records from

1168   the southeast Labrador Sea: ocean circulation changes and ice-rafting events during

1169   the last 160,000 years. *Paleoceanography*, 18 (1), 1018, doi:10.1029/2001PA000736.

1170   Roy, M., Hemming, S.R., Parent, M., 2009. Sediment sources of northern Quebec and

1171   Labrador glacial deposits and the northeastern sector of the Laurentide Ice Sheet

1172   during ice-rafting events of the last glacial cycle. *Quaternary Science Reviews*, 28

1173   (27-28), 3236-3245.

1174   Ryder, J.M. and Clague, J.J., 1989. British Columbia (Quaternary stratigraphy and history,

1175   Cordilleran Ice Sheet). In, Fulton, R.J. (ed), *Quaternary Geology of Canada and*

1176   *Greenland*. Geological Survey of Canada, Geology of Canada, no. 1.

1177   Shackleton, N.J., 1987. Oxygen isotopes, ice volume and sea level. *Quaternary Science*

1178   *Reviews*, 6 (3-4), 183-190.

1179   Shepherd, A., and Wingham, D., 2007. Recent sea-level contributions of the Antarctic and

1180   Greenland ice sheets. *Science*, 315 (5818), 1529-1532.

1181   Shaw, J., Piper, D.J.W., Fader, G.B.J., King, E.L., Todd, B.J., Bell, T., Batterson, M.J.,

1182   Liverman, D.G.E., 2006. A conceptual model of deglaciation of Atlantic Canada.

1183   *Quaternary Science Reviews* 25, 2059–2081.

1184   Skinner, R.G., 1973. Quaternary stratigraphy of the Moose River basin, Ontario. *Geological*

1185   *Survey of Canada, Bulletin*, 225, 77 pp.

1186   St-Onge, D.A., 1987. The Sangamonian Stage and the Laurentide Ice Sheet. *Géographie*

1187   *physique et Quaternaire*, 41 (2), 189-198.

1188   Stokes, C.R., and Clark, C.D., 2001. Palaeo-ice streams. *Quaternary Science Reviews*, 20,

1189   1437-1457.

1190   Stokes, C.R. and Clark, C.D., 2003. Laurentide ice streaming over the Canadian Shield: a

1191   conflict with the 'soft-bedded' ice stream paradigm? *Geology*, 31 (4), 437-350.

1192   Stokes, C.R. and Clark, C.D., 2004. Evolution of Late Glacial ice-marginal lakes on the

1193   north-western Canadian Shield and their influence on the location of the Dubawnt

1194   Lake palaeo-ice stream. *Palaeogeography, Palaeoclimatology, Palaeoecology*, 215,

1195   (1/2), 155-171.

1196   Stokes, C., and Tarasov, L., 2010. Ice streaming in the Laurentide Ice Sheet: A first

1197   comparison between data-calibrated numerical model output and geological evidence.

1198   *Geophysical Research Letters*, 37, L01501.

1199   Stokes, C.R., Clark, C.D., Darby, D.A. and Hodgson, D., 2005. Late Pleistocene ice export

1200   events into the Arctic Ocean from the M'Clure Strait Ice Stream, Canadian Arctic

1201   Archipelago. *Global and Planetary Change*, 49, 139-240.

1202   Stokes, C.R., Clark, C.D. & Winsborrow, M.C.M., 2006. Subglacial bedform evidence for a

1203   major palaeo-ice stream and its retreat phases in Amundsen Gulf, Canadian Arctic

1204   Archipelago. *Journal of Quaternary Science*, 21 (4), 399-412.

1205

1206 Stokes, C.R., Clark, C.D. and Storrar, R., 2009. Major changes in ice stream dynamics during

1207   deglaciation of the north-western margin of the Laurentide Ice Sheet. *Quaternary*

1208   *Science Reviews,* 28 (7-8), 721-738.

1209 Stroeven, A.P., Fabel, D. and Marshall, S., 2002. Inceptions: mechanisms, patterns and

1210   timing of ice sheet inception. *Quaternary International*, 95-96, 1-4.

1211 Tarasov, L., and Peltier, W.R., 1997a. Terminating the 100 kyr ice age cycle. *Journal of*

1212   *Geophysical Research*, 102 (D18), 21,665-21,693.

1213 Tarasov, L., and Peltier, W.R., 1997b. A high resolution model of the 100-kyr ice-age cycle.

1214   *Annals of Glaciology*, 25, 58-65.

1215 Tarasov, L., and Peltier, W.R., 2003. Greenland glacial history, borehole constraints, and

1216   Eemian extent. *Journal of Geophysical Research – Solid Earth*, 108 (B3), 2143, doi:

1217   10.1029/2001JB001731.

1218 Tarasov, L., and Peltier, W.R., 2004. A geophysically constrained large ensemble analysis of

1219   the deglacial history of the (North American) ice sheet complex. *Quaternary Science*

1220   *Reviews*, 23, 359-388.

1221 Tarasov, L., and Peltier, W.R., 2005. Arctic freshwater forcing of the Younger Dryas cold

1222   reversal. *Nature*, 435 (7042), 662-665.

1223 Tarasov, L., and Peltier, W.R., 2007. The co-evolution of continental ice cover and

1224   permafrost extent over the last glacial-interglacial cycle in North America. *Journal of*

1225   *Geophysical Research – Earth Surface*, 112, F02S08.

1226 Tarasov, L., Dyke, A.S., Neal, R.M. and Peltier, W.R., 2012. A data-calibrated distribution of

1227 deglacial chronologies for the North American ice complex from glaciological

1228 modelling. *Earth and Planetary Science Letters*, 315-316, 30-40.

1229 Veillette, J.J., 2004. Ice-flow chronology and palimpsest, long-distance dispersal of indicator

1230 clasts, north of the St. Lawrence River Valley, Quebec. *Géographie physique et*

1231 *Quaternaire*, 58 (2-3), 187-216.

1232 Veillette, J.J., Dyke, A.S. and Roy, M., 1999. Ice-flow evolution of the Labrador Sector of

1233 the Laurentide Ice Sheet: a review, with new evidence from northern Quebec.

1234 *Quaternary Science Reviews*, 18, 993-1019.

1235 Vincent, J-S., Prest, V.K., 1987. The Early Wisconsinan history of the Laurentide Ice Sheet.

1236 *Géographie physique et Quaternaire*, 41 (2), 199-213.

1237 Waelbroeck, C., Labeyrie, L., Michel, E., Duplessy, J., McManus, J., Lambeck, K., Balbon,

1238 E. and Labracherie, M., 2002. Sea-level and deep water temperature changes derived

1239 from benthic foraminifera isotopic records. *Quaternary Science Reviews*, 21 (1-3),

1240 295-305.

1241 Williams, L.D., 1978. Ice-sheet initiation and climatic influences of expanded snow cover in

1242 Arctic Canada. *Quaternary Research*, 10, 141-149.

1243 Williams, L.D., 1979. An energy balance model of potential glacierization of northern

1244 Canada. *Arctic and Alpine Research*, 11, 443-456.

1245 Winsborrow, M., Clark, C.D. and Stokes, C.R., 2004. Ice streams of the Laurentide Ice Sheet.

1246 *Géographie physique et Quaternaire*, 58 (2-3), 269-280.

1247 Winsborrow, M., Clark, C.D. and Stokes, C.R., 2010. What controls the location of ice

1248 streams? *Earth-Science Reviews*, 103 (1-2), 45-59.

1249   Wohlfarth, B., 2010. Ice-free conditions in Sweden during Marine Oxygen Isotope Stage 3?

1250   *Boreas*, 39 (2), 377-398.

1251   Wolken, G.J., England, J. and Dyke, A.S., 2005. Re-evaluating the relevance of vegetation

1252   trimlines in the Canadian Arctic as an indicator of the Little Ice Age

1253   paleoenvironments. *Arctic*, 58, 341-353.

1254   Wolken, G.J., England, J. and Dyke, A.S., 2008. Changes in Neoglacial perennial snow/ice

1255   extent and equilibrium line altitudes in the Queen Elizabeth Islands, Arctic Canada.

1256   *The Holocene*, 18, 615-627.

1257 **Tables:**

1258 **Table 1:** Pre-LGM ice volume metric components. Maximum ice volume over the given time

1259 interval was tested against the constraint. Both the un-penalized range and maximum ice

1260 volume accepted are shown in m eustatic equivalent of ice. Runs with ice volumes below the

1261 un-penalized range are rejected. Weaker versions of the 37-33 and 50-42 ka constraints

1262 (respectively at 30 and 49 ka) were part of the original calibration.

1263

Time (ka)	Un-penalised range (m)	Maximum accepted
115 to 105	21-36	40
93-84	8-34	40
67-57	47-65	71
50-42	49-63	67
37-33	50-65	70

1264

1265

1266

Figure Captions:

Figure 1: Map of the 'basal flow factor' used as input for the Glacial Systems Model. A value of zero represents a grid cell where fast flow due to subglacial till deformation is not permitted. The strength of fast flow due to subglacial till deformation and hard-bedded sliding are both subject to calibration.

Figure 2: Climate forcing interpolation index between present-day observed (value 0) and LGM climate (value 1). 'Original' is a glaciological inversion of the GRIP and GISPII records (updated from Tarasov and Peltier, 2003), now with the gicc05 chronology for GRIP (NGRIP dating group, 2006). This time series was used for the calibration. The 'deformed' time series is the temporally adjusted version to attain an approximate match to the inferred sea level record from Waelbroeck *et al.* (2002) and is an advance on previous work (e.g. Tarasov and Peltier, 1997a; b)

Figure 3: Ensemble probability plots of ice thickness >1 m at 120 ka, 118 ka, 116 ka, 114 ka and 112 ka.

Figure 4: Evolution of modelled weighted ensemble average of basal velocity for the North American Ice Sheet Complex during major OIS stages at 110 ka (5d), 100 ka (5c), 90 ka (5b), 80 ka (5a), 65 ka (4), 55 ka (early 3), 40 ka (mid 3) and 25 ka (2: ~LGM). For clarity, mean surface elevation contours are at 200 m intervals except for bathymetry and areas under 400 m. The thick light blue line is the ice margin. White areas are at or near to cold-based conditions.

Figure 5: (a) Modelled ice sheet volume of the North American Ice Sheet Complex from the last interglaciation to the LGM in eustatic equivalent meters of sea level (conversion factor of 25.19 m per 10^{15} m^3 of ice) and, (b), corresponding ice sheet volume change expressed as rate of metres of sea level equivalent. All ages are calendar yr BP. Mean and two sigma deviation ranges from the calibrated ensemble are shown.

Figure 6: Ensemble distribution of the fraction of warm-based based ice over time. 'Old ensemble' is from Tarasov and Peltier (2007), which did not apply pre-LGM constraints on ice volume and used the 'original' climate interpolation function in Figure 2, contrary to 'new ensemble' from current study.

Figure 7: Pre-LGM time series' of maximum basal velocity near the margin for four fast flow zones that correspond to the location of 'known' ice streams during deglaciation (cf. Patterson, 1998; Stokes and Clark, 2001; Winsborrow *et al.*, 2004; see also Fig. 9): (a) Hudson Strait, (b), M'Clure Strait, (c) Gulf of St Lawrence, and (d), Des Moines Lobe. Weighted ensemble mean and one standard deviation uncertainties are shown. To minimize flux loss from ablation in the calculations, velocities were computed one grid cell in from the ice marginal cell (terrestrial) or at grid cells with grounded ice adjacent to floating ice. Fluxes were computed using basal ice velocities to isolate the contribution from streaming as opposed to ice deformation.

Figure 8: (a) Possible extent of the Laurentide Ice Sheet in pre-Middle (Early?) Wisconsinan time based on an extensive review of geological evidence by Vincent and Prest (1987). Although some of the evidence used to reconstruct this ice margin has been subsequently re-

1315   interpreted (e.g. England *et al.*, 2009), the margin position is almost identical to our modelled

1316   Early Wisconsinan ice sheet at 65 ka (see Fig. 4).   (b) Possible maximum extent of the

1317   Middle Wisconsinan ice sheet based on an extensive review of geological evidence by

1318   Dredge and Thorleifson (1987). Dredge and Thorleifson (1987) acknowledge uncertainty

1319   over the precise extent of the ice sheet during OIS 3 and also discuss more minimal

1320   configurations. However, the maximum configuration shown here is entirely consistent with

1321   our relatively large ice sheet between ca. 45 and 50 ka (Fig. 4).

1322

1323   **Figure 9:** Correspondence between modelled fast flow features at 40 ka and locations where

1324   ice streams are known to have existed during the deglacial interval. Clockwise: HS = Hudson

1325   Strait (e.g. Andrews and MacLean, 2003), LS = Lancaster Sound (e.g. Klassen and Fisher,

1326   1988; De Angelis and Kleman, 2007), MS = Massey Sound (e.g. England *et al.*, 2006); M'CS

1327   = M'Clure Strait (e.g. Stokes *et al.*, 2005); AG = Amundsen Gulf (e.g. Stokes *et al.*, 2006),

1328   MT = Mackenzie Trough (e.g. Beget, 1987), CP = Canadian Prairies (e.g. O'Cofaigh *et al.*,

1329   2010), DM = Des Moines Lobe (e.g. Patterson, 1997), LM = Lake Michigan Lobe (e.g.

1330   Kehew *et al.*, 2005)

1331

1332   **Figure 10:** (a) Total flux from all streaming (>500 m/yr) cells at the margin of the grounded

1333   part of ice-sheet through time and, (b), relative area of streaming through time (grid cells

1334   >500 m/yr). Both show ensemble mean, one standard deviation, and results for one of the

1335   best scoring model runs (nn9925). Note that streaming flux increases through time towards

1336   the LGM and is largely modulated by ice sheet volume, see also Fig. 11,

1337

1338   **Figure 11**: Total flux from all streaming (>500 m/yr) cells at margin of grounded part of ice-

1339   sheet through time as a function of ice volume. Mean ensembles results were decomposed

1340   into growth and decay sequences and the 29 ka to 20 ka interval was excluded because of the

1341   dynamic facilitation of H-events (see section 3.3). These plots demonstrate the strong

1342   dependence of ice stream activity on ice sheet volume with no marked dependence on

1343   whether the ice sheet is in a growth or decay stage except at ice volumes greater than about

1344   55 m eustatic equivalent.
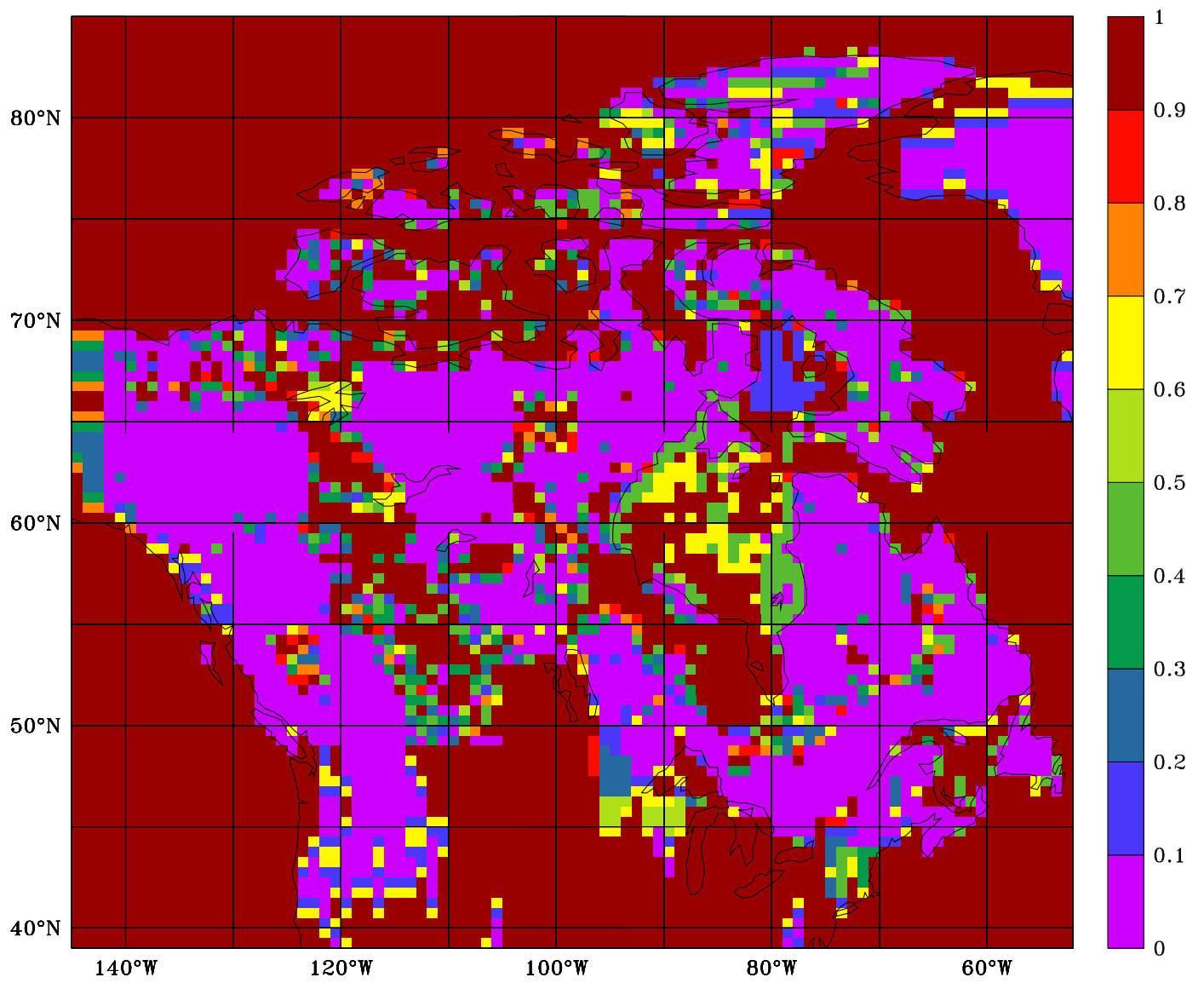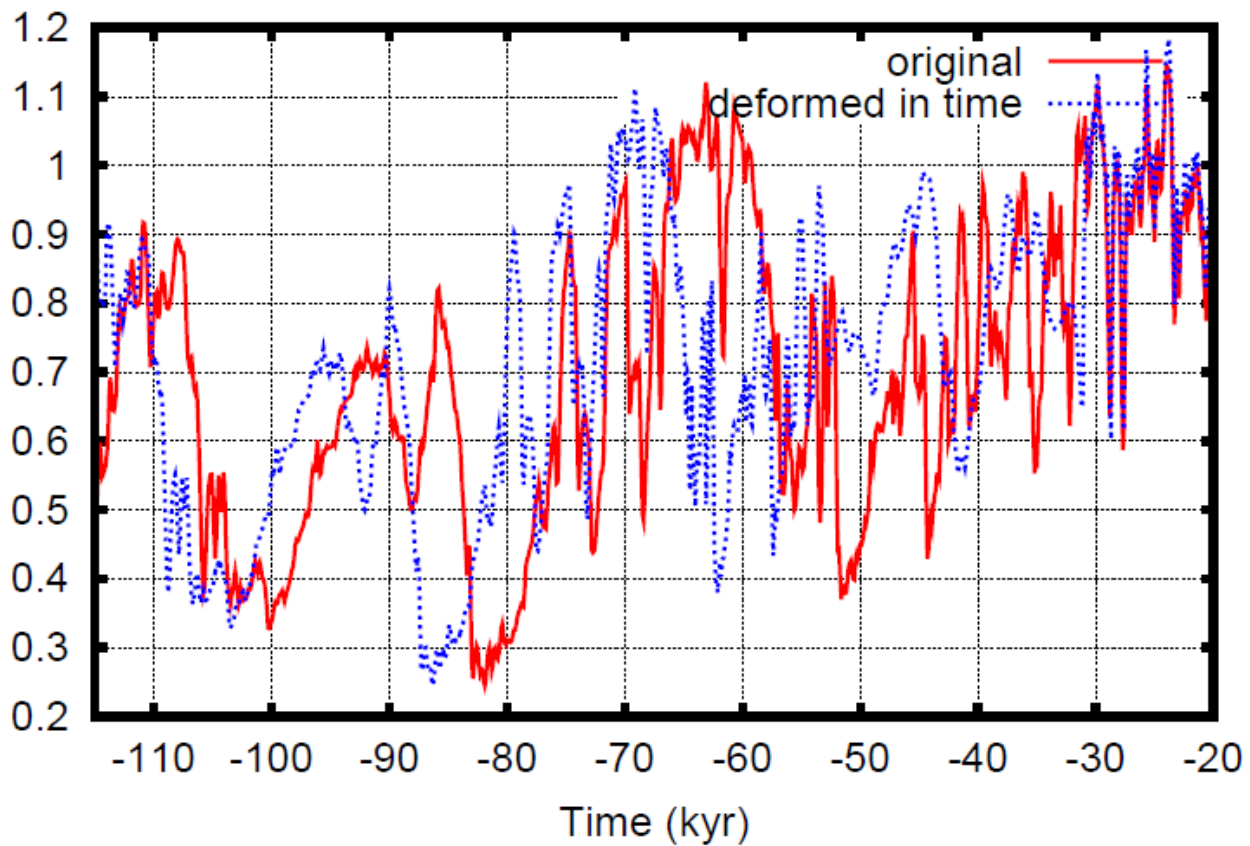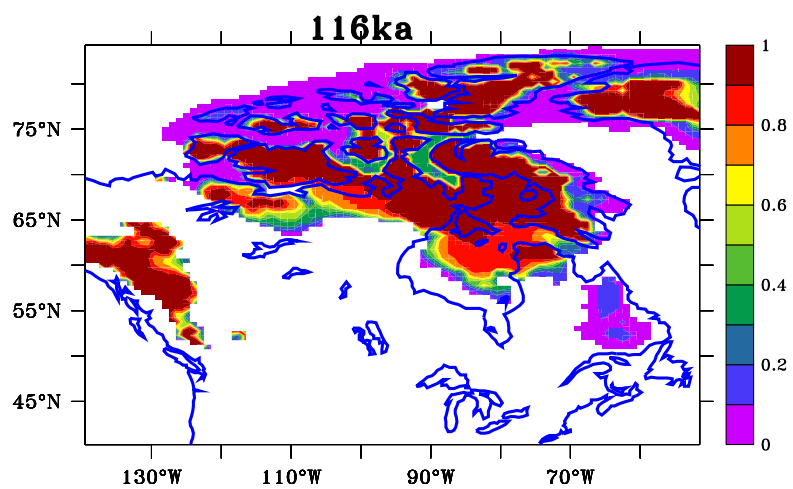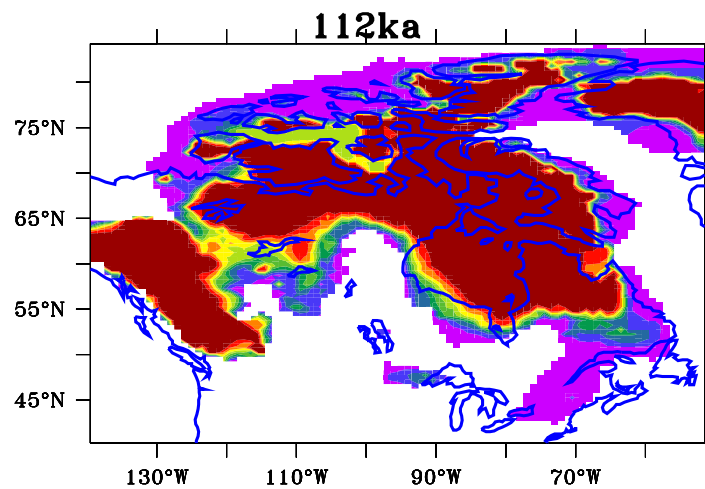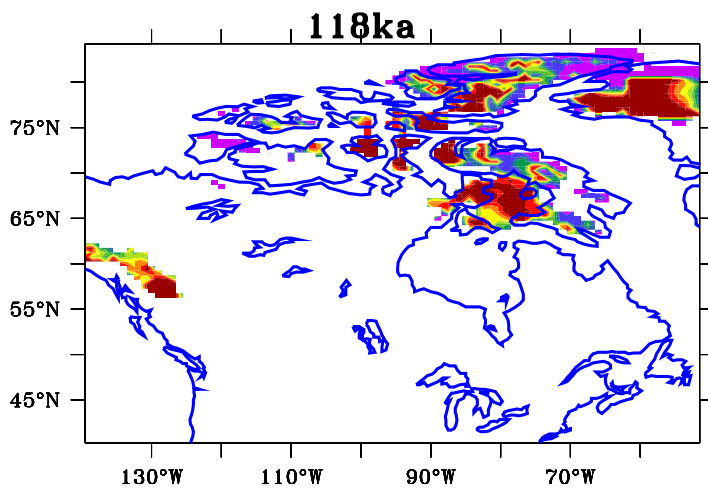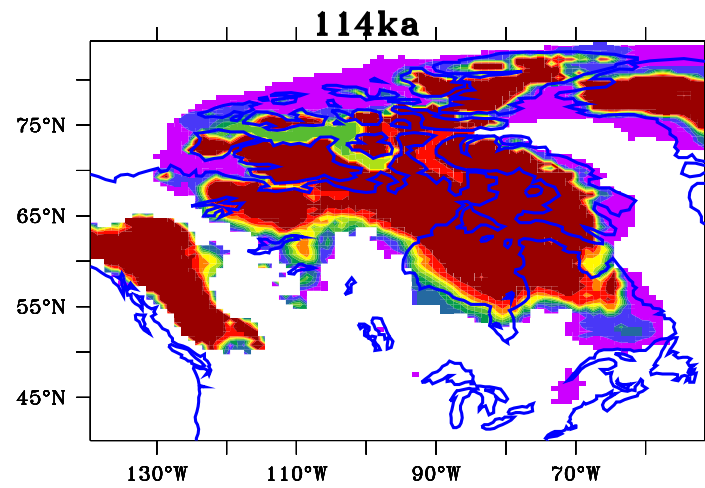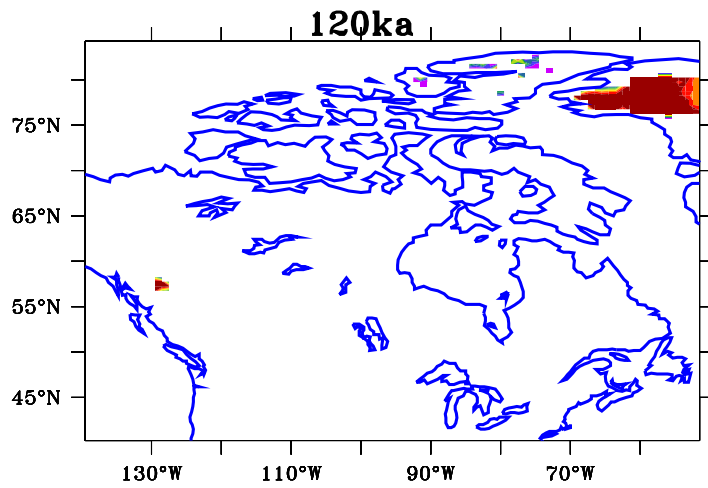
Figure 2

−110ka (5d)
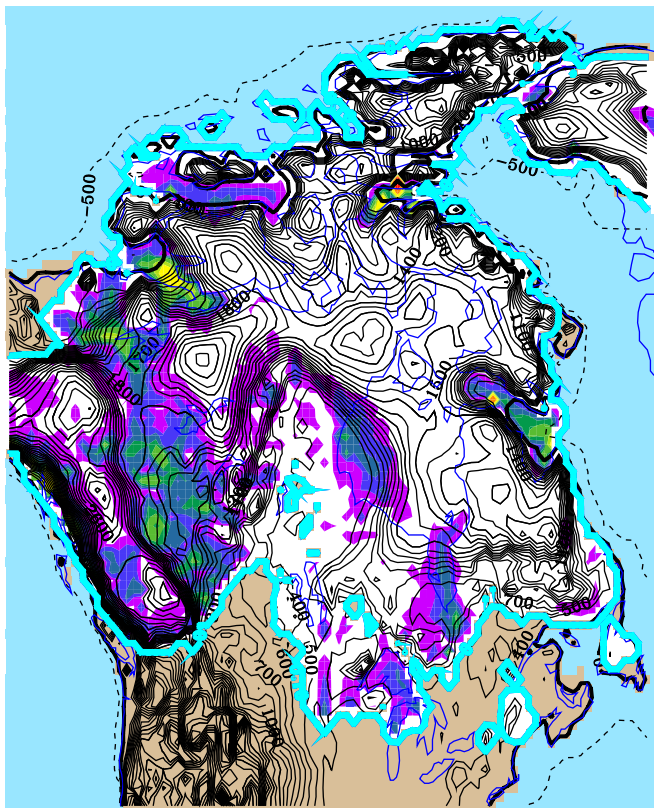
−100ka (5c)
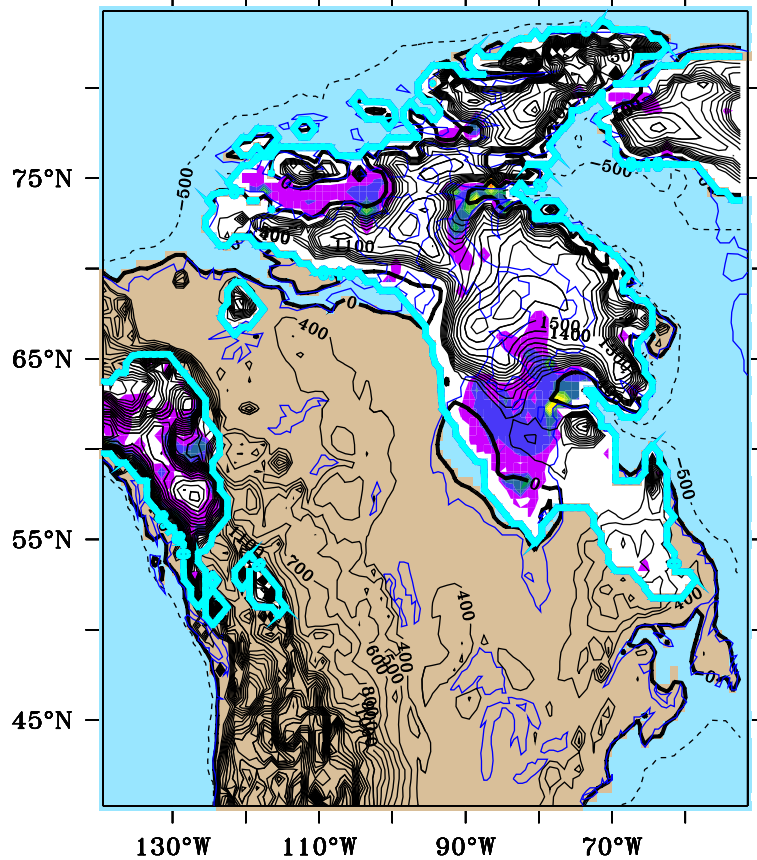
−90ka (5b)
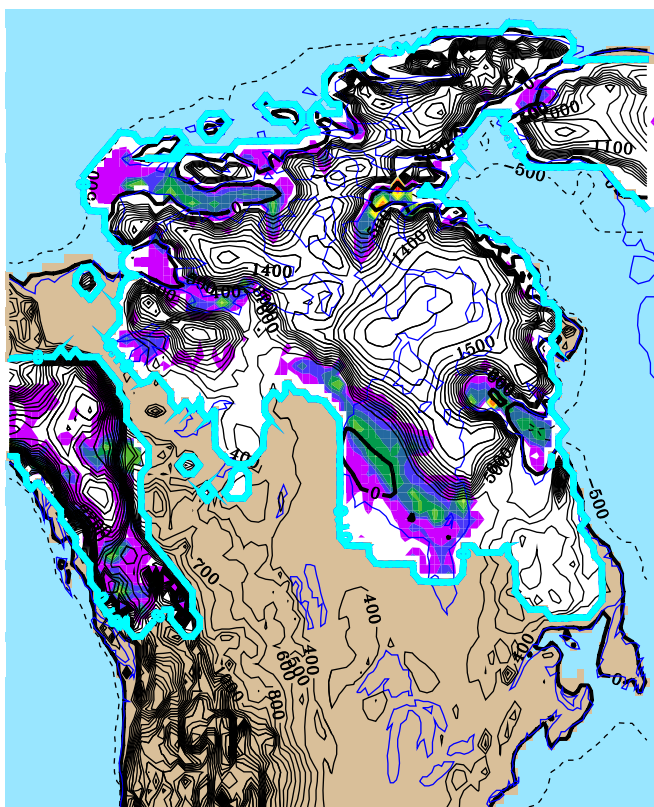
−80ka (5a)
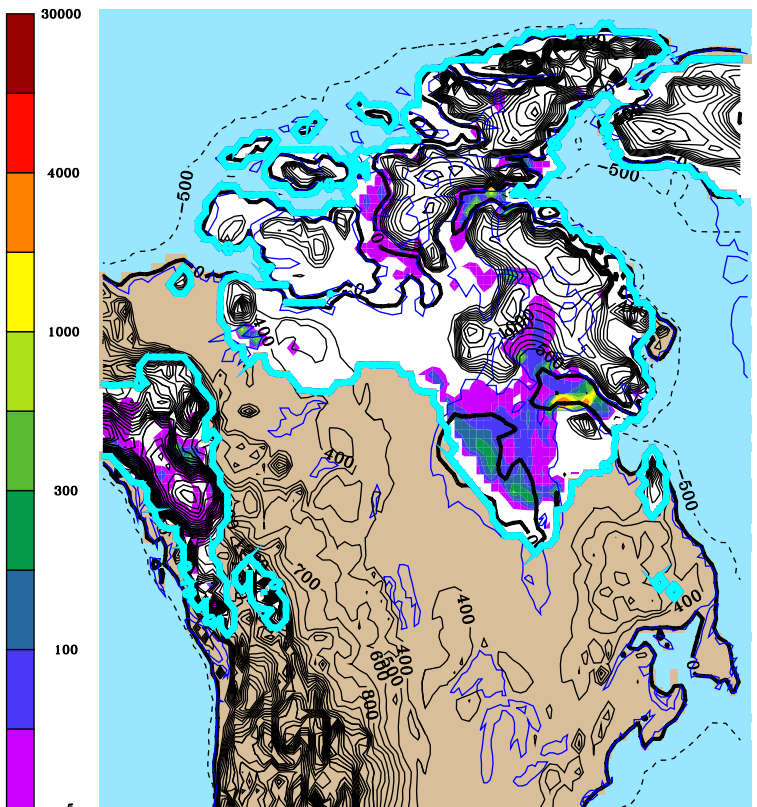
(m/yr)

-65ka (4)
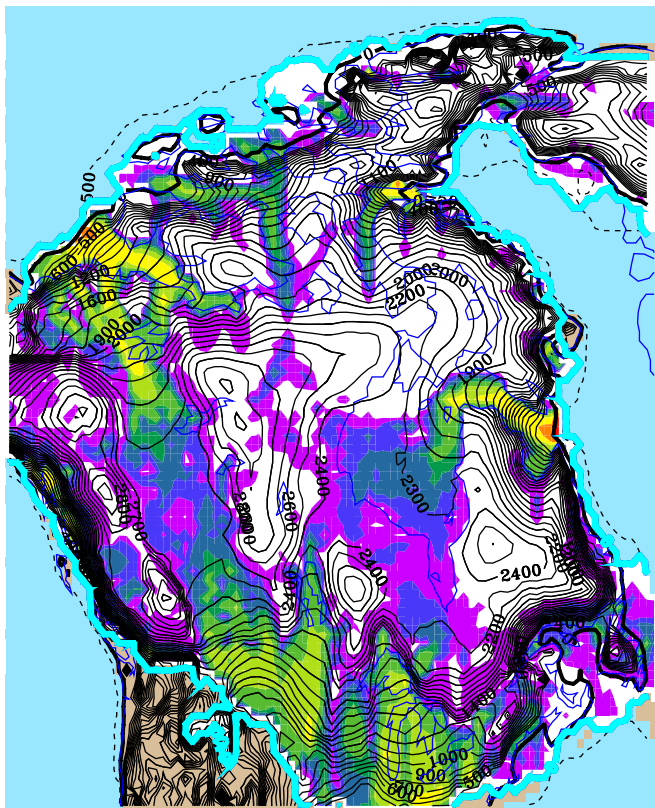
-55ka (early 3)
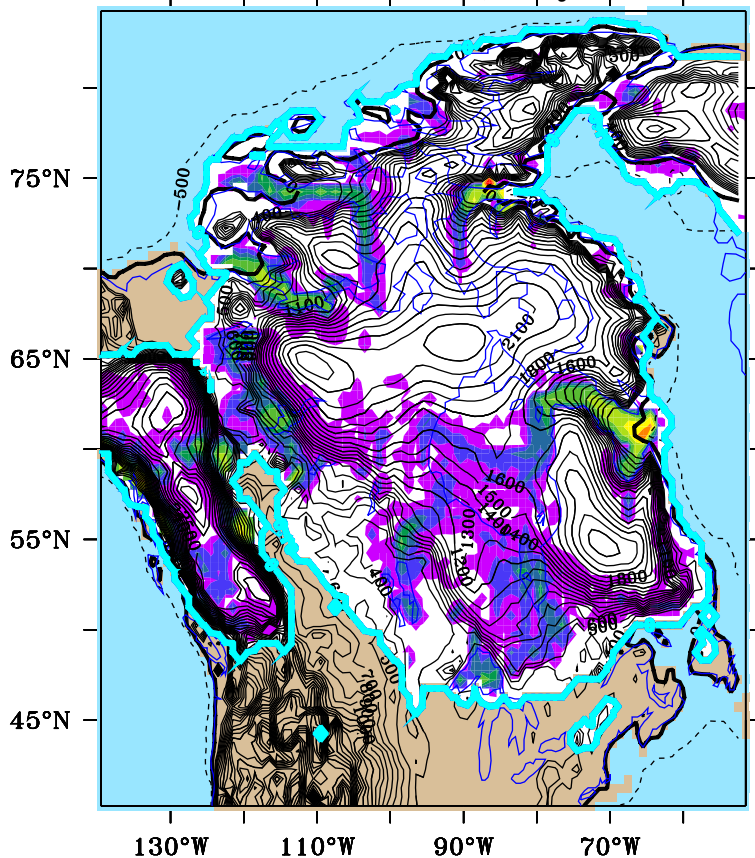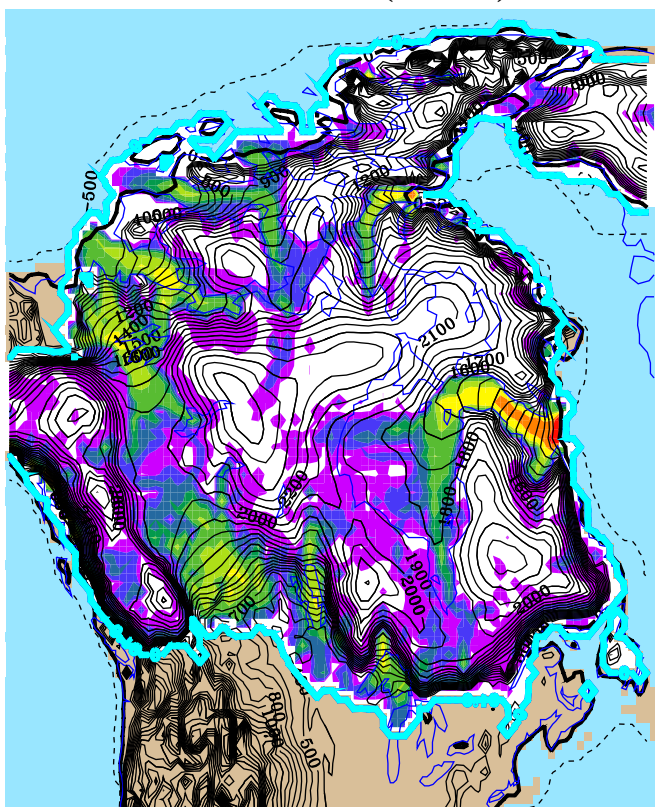
-40ka (mid 3)

-25ka (2: LGM)
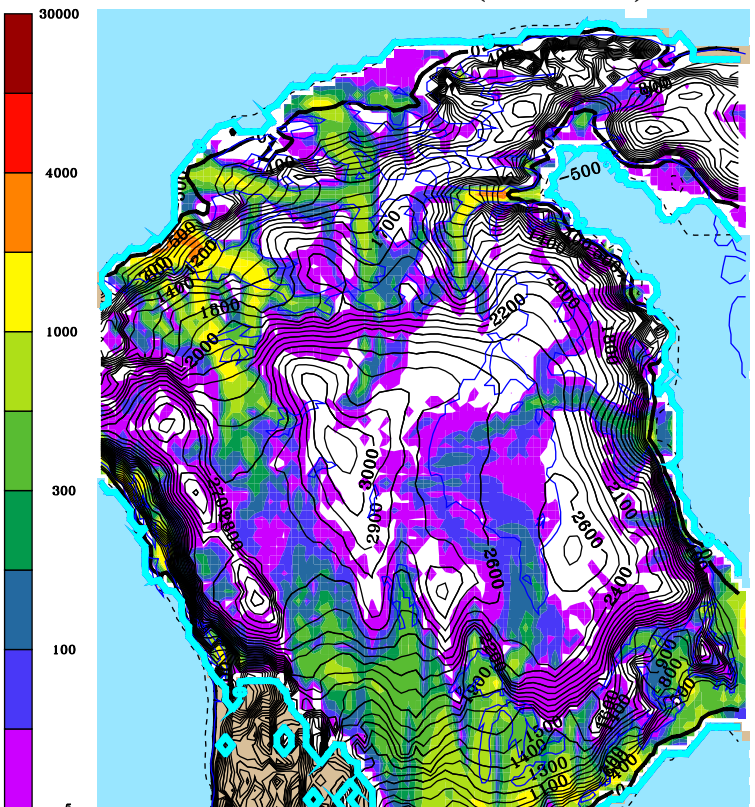
(m/yr)
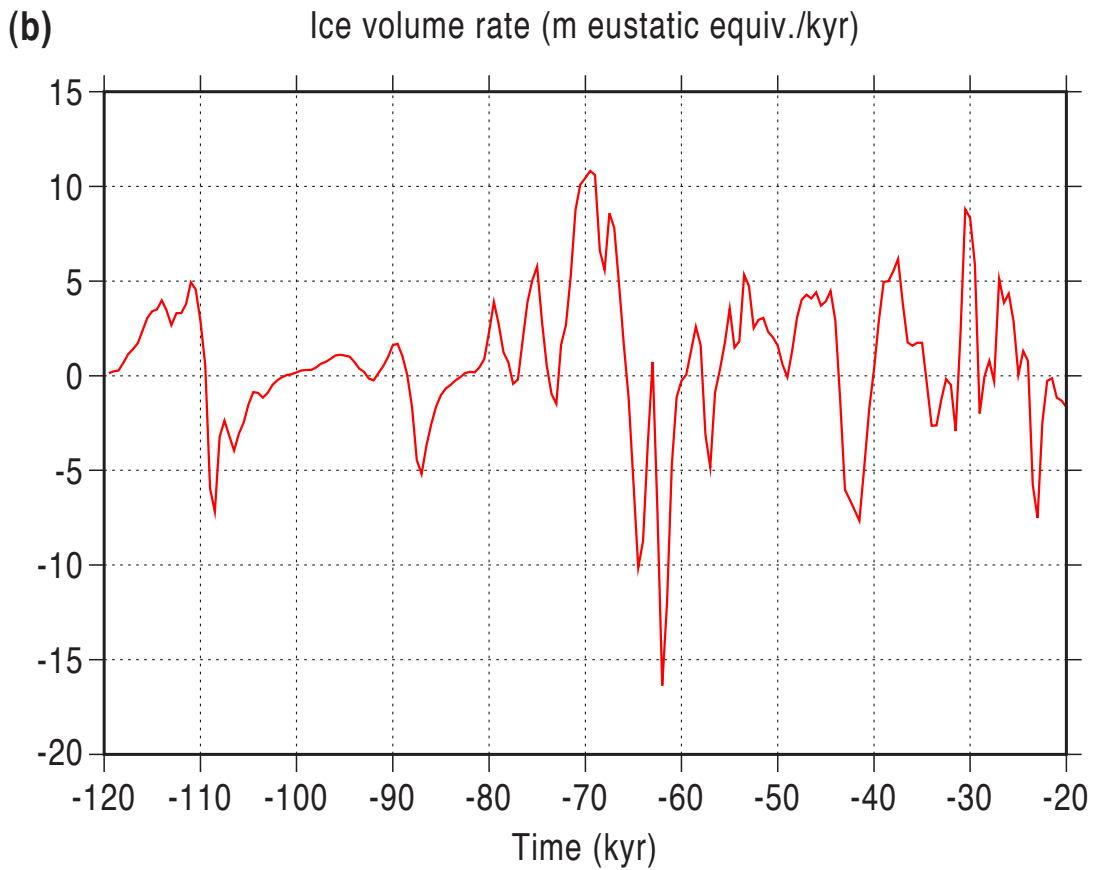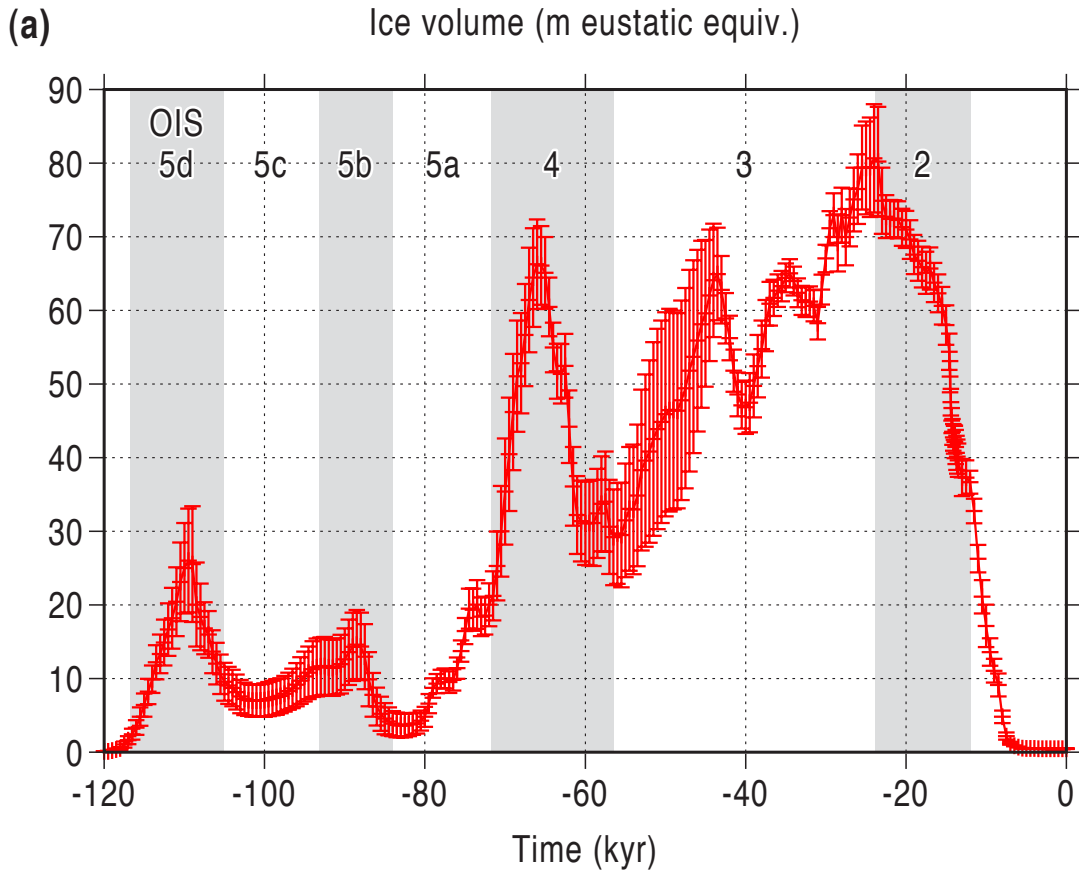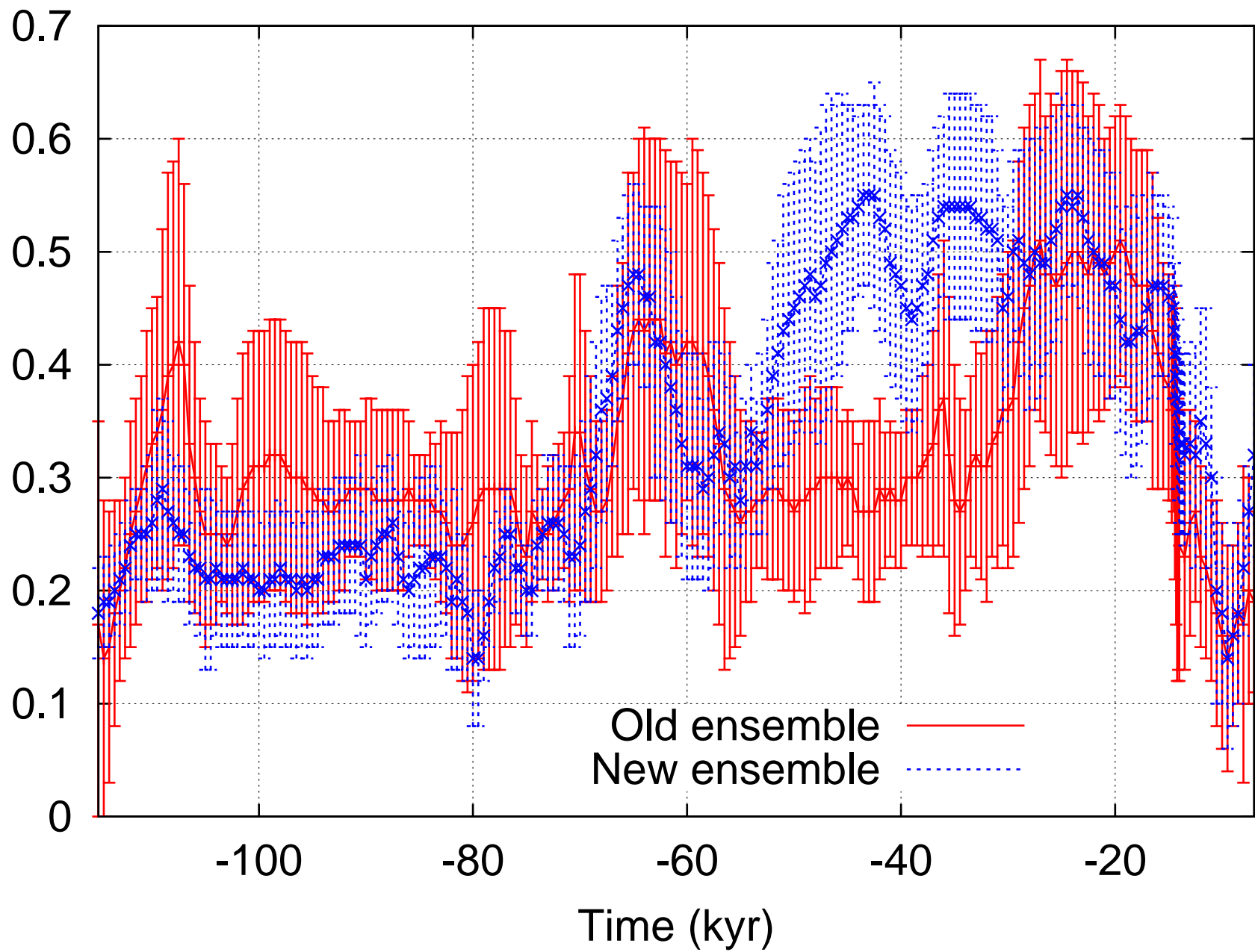
(a) Ice volume (m eustatic equiv.)
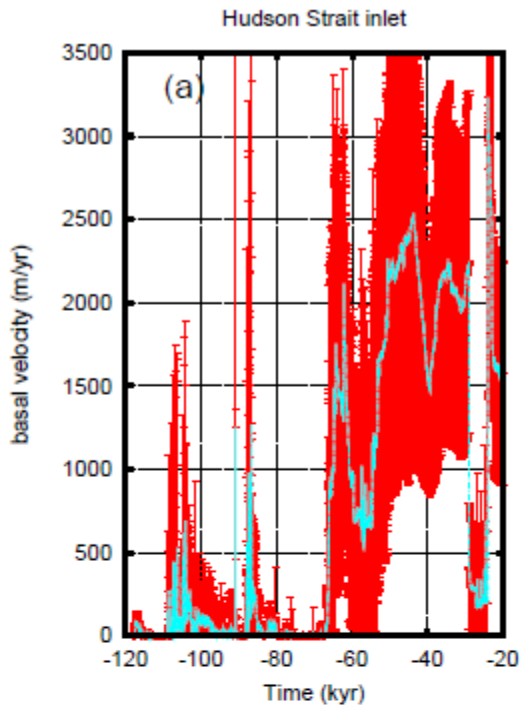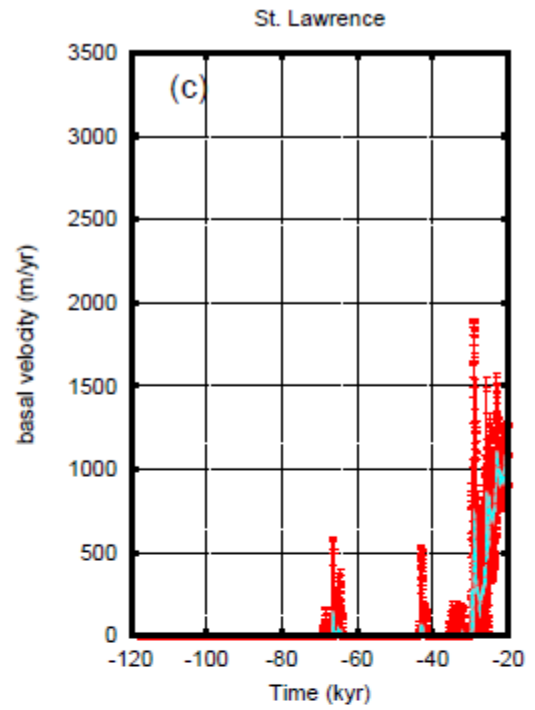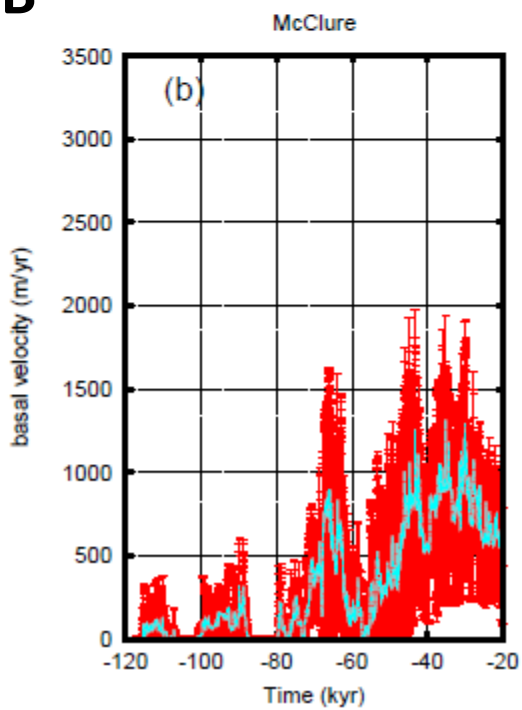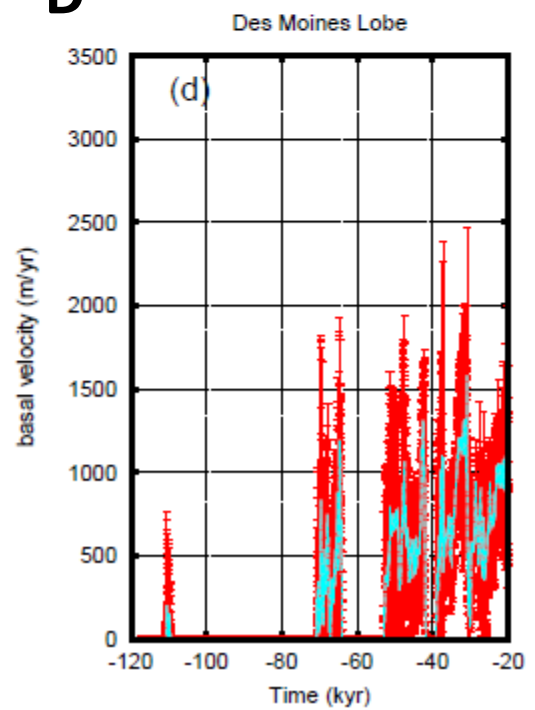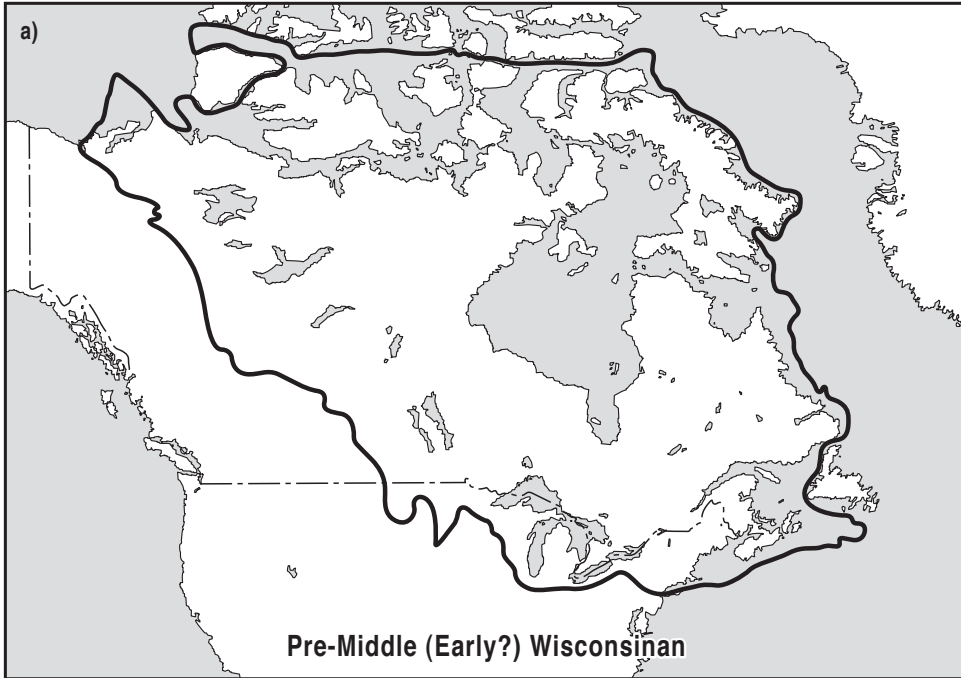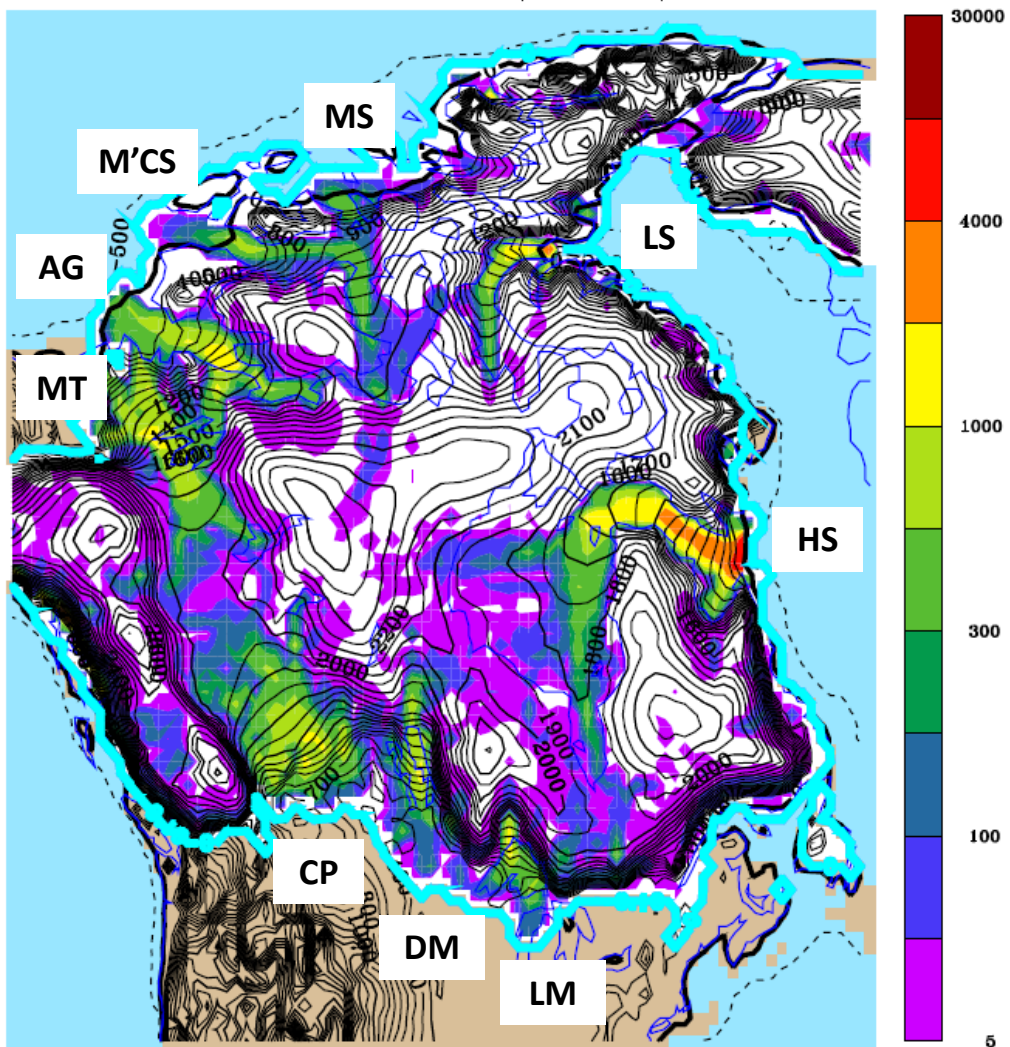
(b) Ice volume rate (m eustatic equiv./kyr)

A Hudson Strait inlet

B McClure

C St. Lawrence

D Des Moines Lobe

Figure 7

a) Pre-Middle (Early?) Wisconsinan

b) Middle Wisconsinan

Figure 9

(a) Grounded margin stream flux (* 10^3 km^3/yr)

mean
nn9925

(b) Relative area of streaming

mean
nn9925
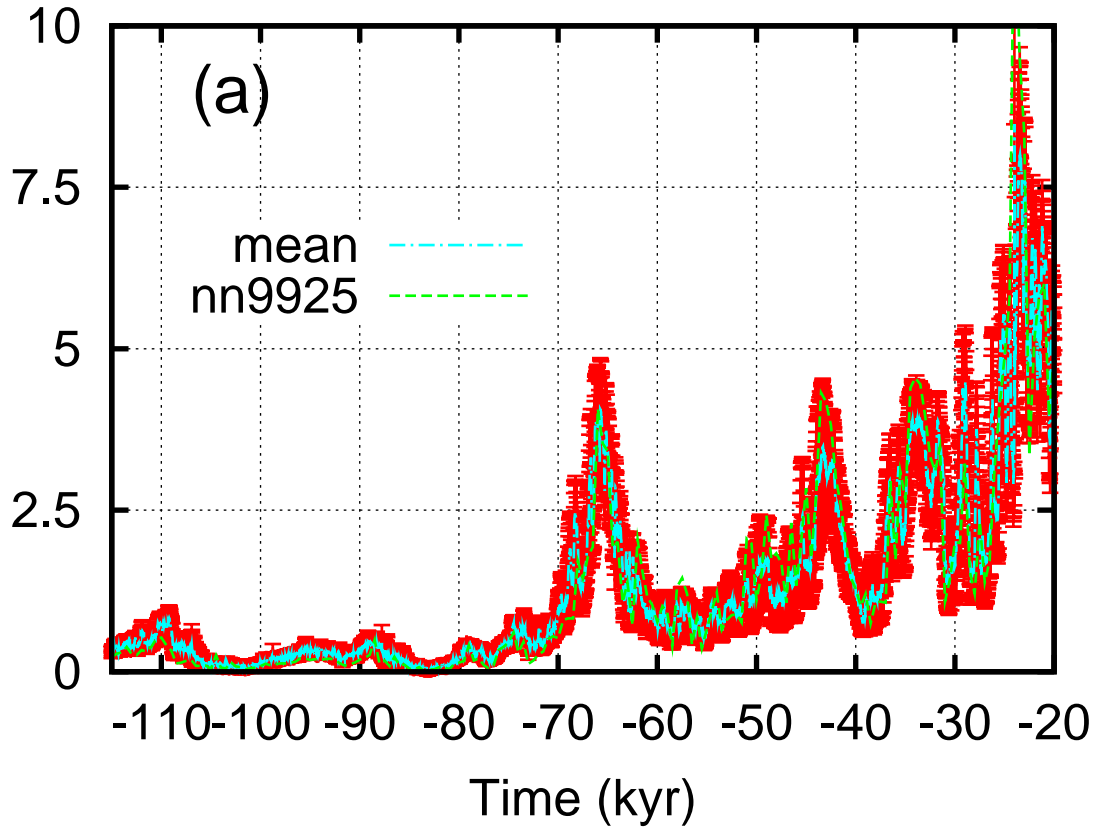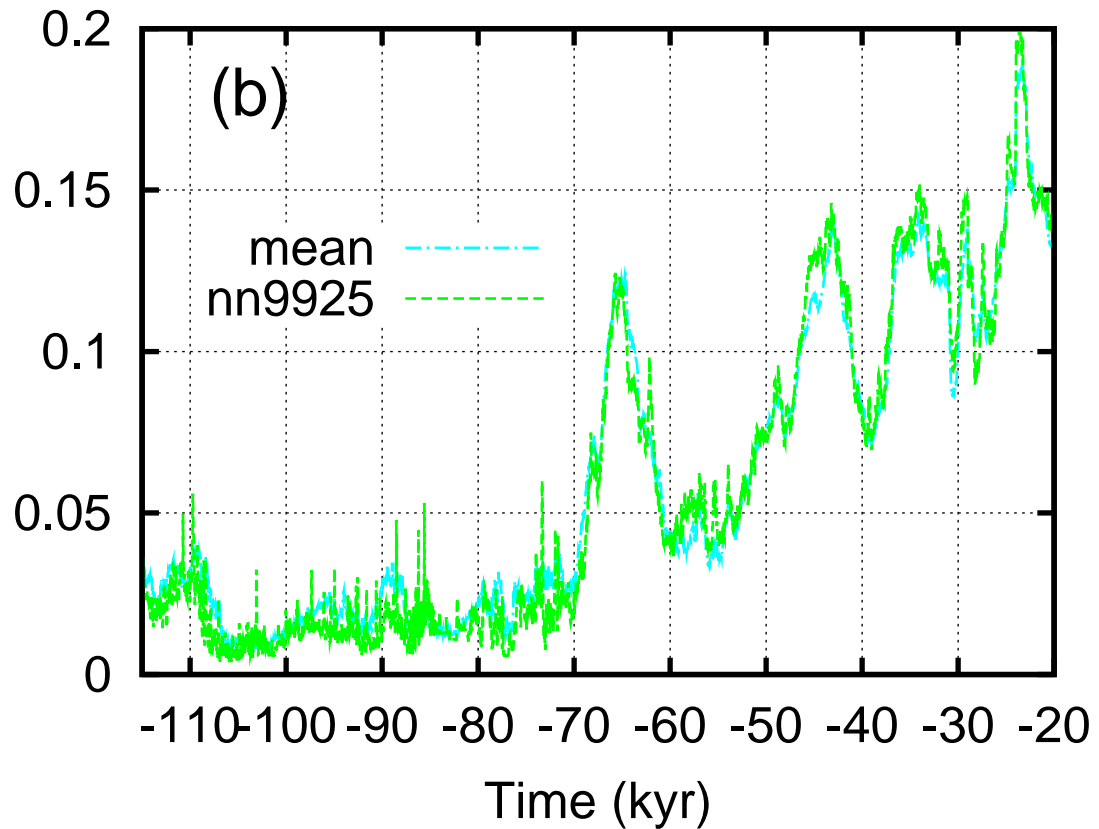
grounded margin stream flux/volume ($* 10^{-5}$ yr^{-1})

(a)

mean
nn9925 streaming flux
nn9925, 3kyr running avg

Time (kyr)

grounded margin stream flux ($* 10^3$ km^3/yr)

(b)

decay, exponent 2.6
growth, exponent 2.3

ice volume (m eustatic equivalent)